

ISBN 82-553-0799-0
Applied Mathematics

No 1
January 1993

Nonlinear modulations of a solitary wave

by
Geir Pedersen

PREPRINT SERIES – Matematisk institutt, Universitetet i Oslo



Nonlinear modulations of a solitary wave.

Geir Pedersen

December 21, 1992

Abstract

The leading approximation to slowly varying solitary crest on constant depth is the plane soliton solution substituted the local values of amplitude and orientation. This leads two nonlinear hyperbolic equations for the local amplitude and inclination of the crest that have been reported by several authors and predict the formation of progressive wave jumps, or shocks, from any initial perturbation of the crest. In comparison to numerical solutions of the Boussinesq equations we find that this optical approximation fails to reproduce essential properties of the crest dynamics, in particular that the crest modulations are damped and well defined wave jumps do not necessarily evolve. One purpose of the present work is to include such features in an amended optical approximation.

We obtain the leading correction to the “local soliton” solution by a multiple scale technique. In addition to a modification on the wave profile the perturbation expansion also yields a diffracted wave system and a celerity speed that depend on the curvature of the crest. The energy conservation arguments then lead us to a second order optical approximation consisting of transport equations of mixed hyperbolic/parabolic nature. Under additional assumptions the transport equations can be reduced to the well known Burgers equation.

Numerical simulation of the Boussinesq equations are performed for modulations on otherwise straight crests and radially converging solitons. The improved optical, or ray, theory reproduce all essential features and agree closely with the numerical solution in both cases. Contrary to standard purely hyperbolic optical description the present theory also predict wave jumps of finite width that are consistent with the triad solution of Miles (1977).

The present work indicates that while sinusoidal waves often are appropriately described by the lowest order physical optics, higher order corrections must be expected to be important for single crested waves.

Contents

1	Introduction	3
2	Basic equations	4
2.1	Long wave equations	4
2.2	The soliton solution	6
3	Perturbation solutions for slow variation and ray equation	6
3.1	Simple ray theory	7
3.2	Formulation of the perturbation expansion, kinematic equations . . .	8
3.3	The first order solution.	11
3.4	Uniformity and diffracted wave field	14
3.5	Perturbations on straight crests	14
3.6	The axisymmetric case	15
4	Application of conservation laws.	17
4.1	Integrated conservation laws	17
4.2	The higher order energy equation.	19
4.3	Higher order ray theory for nearly straight crests.	20
4.4	Higher order equations for radially converging waves	22
5	Examples	23
5.1	A self-similar perturbation – comparison to the Boussinesq equations	24
5.2	Wave jump – comparison to Miles solution	31
5.3	Axisymmetric converging waves	34
6	Concluding remarks	39
A	Numerical solution of the ray equations	40

1 Introduction

Waves moving in a slowly varying bathymetry or on a gently varying current will locally behave approximately as if in a homogeneous medium. Likewise, nonlinear waves with a slowly varying amplitude and orientation may locally behave as a plane wave of constant amplitude. Naturally, this will be useful, or make sense at least, only if the wave can be appropriately recognized as belonging to a well defined class with known properties concerning propagation speed, energy density etc. Assumptions on slow variation, in the above sense, is the basis of a series of physical concepts as well as theoretical approaches and techniques. These are most extendedly developed and applied for harmonic linear waves, but there has also been some progress for particular species of nonlinear waves as shock waves (Whitham 1974), Stokes type waves (Peregrine 1985) and shallow water solitons (Miles 1980) which are the concern of the present work.

Seismic activity, submarine slides, rock and snow avalanches into lakes etc. may generate devastating systems of huge waves. In coastal waters these may be headed by one or more crest of a form akin to solitary waves. Hence, insight into the dynamics of nonuniform solitary crests may be helpful for the understanding of tsunami propagation and impact on shore. As demonstrated by the inverse scattering technique, shallow water solitons have a strong tendency to emerge from a variety of initial conditions, besides being stable. This gives confidence that a crest may remain soliton like while influenced by a varying topography or an inherent lateral amplitude variation, and that solitary wave crests, carrying the major part of the total energy, finally may emerge even after substantial distortion. Hence, approximately soliton shaped crests should be well suited for ray theory. The larger part of the reported work in the field has been directed to solitons normally incident on a shelf or propagating in a channel of narrow, but gently varying, width. However, there have also been some activity on genuine three dimensional problems, generally through application of simple optical methods. Kulikovskii & Reutov (1976,1980) studied solitons in variable depths and over under-water trenches and ridges. Reutov (1976) and Miles (1977c) discuss the behavior of nonuniform solitary crests in constant depth. One of the major results is the existence of laterally moving disturbances, as a sort of secondary waves, that eventually develop shocks. Analogous shocks, or wave jumps, are known also for other nonlinear waves (Peregrine 1983, Yue & Mei 1980, Liu & Yoon 1986). For shallow water solitons Miles (1977b) gives a complete description of such jumps in form of phase locked triads, presented in the context of Mach reflection. Herein we will investigate the dynamics of a solitary crest both through general numerical solutions and a new optical theory.

A direct derivation of an optical theory for solitons by application of the phase velocity – amplitude relation and the usual assumption concerning energy transport is straightforward. Grimshaw (1970) developed transport equations by means of a formal multiple scale expansion on a set of two dimensional Boussinesq type equations. In 1971 he generalized the expansion to three dimensions, starting this time from the full inviscid description. Later Ko & Kuehl (1979) applied a similar method for radially converging and diverging ion acoustic waves in two and three dimensions. In the present paper we investigate the dynamics of a soliton like crest in constant depth, with the combined purpose of getting insight to the physics as well as the performance of the optical approaches. We find that the standard optical theory, as

described by Miles (1977c), Reutov (1976) and others, displays severe shortcomings when compared to numerical solutions of the Boussinesq equations. This is the main motivation for the construction of a higher order ray theory that is to be presented herein. The corrected transport equations are found by combining a formal perturbation expansion and energy arguments. The expansion is closely related to the one reported by Grimshaw, but is amended in several ways to obtain suitable representations of the higher order terms. When the corresponding modified wave field replace the “local soliton” approximation in the energy balance considerations we then arrive at an improved energy transport equation. A higher order kinetic equation, on the other hand, follow directly from the perturbation technique. Together these two transport equations form an optical approximation that possess important new properties and reproduce full solutions closely in several examples. In the present context the term full means that no assumption of slow variation has been invoked and we apply both numerical solutions of the Boussinesq equations and Miles (1977b) analytical solution for a resonant triad of solitons.

2 Basic equations

Marking dimensional quantities by a star we introduce a coordinate system with horizontal axes ox^* , oy^* in the undisturbed water level and oz^* pointing vertically upwards. Further we assume a flat bottom at $z^* = -h_0^*$ and denote a typical wavelength and wave height by L^* and αh_0^* respectively. Applying different scalings for “vertical” and “horizontal” coordinates, as described by Friedrichs (1948), Laitone (1960) and others we are then led to the following definition of non-dimensional variables:

$$\left. \begin{aligned} x^* &= L^*x & y^* &= L^*y & t^* &= L^*(gh_0^*)^{-\frac{1}{2}}t \\ \eta^* &= \alpha h_0^*\eta & \phi^* &= \alpha L^*(gh_0^*)^{\frac{1}{2}}\phi & z^* &= h_0^*z \end{aligned} \right\} \quad (1)$$

where η is the surface elevation and ϕ the velocity potential. The above scaling is used exclusively in the present section. In the rest of the article both the relative stretch of the vertical coordinates and the extraction of the amplitude factor α become inconvenient and are therefore omitted.

2.1 Long wave equations

Long wave equations are generally developed through expansions in the small parameters α and $\epsilon \equiv (h_0^*/L^*)^2$. We will give a brief sketch of a derivation of a particular set of higher order shallow water equations. In the present scaling the non-dimensional Laplacian equation reads:

$$\epsilon \nabla^2 \phi + \phi_{zz} = 0 \quad (2)$$

where ∇ is the horizontal component of the dimensionless gradient operator and the indices denote partial differentiation. When the quantities also carry other indices those corresponding to differentiation will be preceded by a comma. Following a common approach, first introduced by Boussinesq (1872), we expand ϕ in powers of z . Utilizing the kinematic boundary condition at $z = -1$ we then find:

$$\phi = \sum_{n=0}^{\infty} \epsilon^n (z+1)^{2n} \phi_n(x, y) \quad \text{where} \quad 2n(2n-1)\phi_n = -\nabla^2 \phi_{n-1} \quad \text{for} \quad n \geq 1 \quad (3)$$

Equations for the remaining unknown in this expansion, ϕ_0 , and η can easily be derived from Eulers pressure equation at the free surface and the vertically integrated continuity equations. There are a variety of choices for the final dependent variables. In the present paper we use the depth averaged potential:

$$\bar{\phi} = (1 + \alpha\eta)^{-1} \int_{-1}^{\alpha\eta} \phi dz \quad (4)$$

which is readily related to ϕ_0 through (3). Inverting this relation and substituting the results into the Euler and integrated pressure equations and performing some tedious manipulation we obtain:

$$\eta_t = -\nabla \cdot \{(1 + \alpha\eta)\nabla\bar{\phi} + \frac{\alpha\epsilon}{3}\nabla^2\bar{\phi}\nabla\eta\} + O(\epsilon^2\alpha, \epsilon\alpha^2) \quad (5)$$

$$\begin{aligned} \bar{\phi}_t + \eta + \frac{\alpha}{2}(\nabla\bar{\phi})^2 - \frac{\epsilon}{3}\nabla^2\bar{\phi}_t \\ + \alpha\epsilon\left(\frac{1}{6}(\nabla^2\bar{\phi})^2 - \frac{2}{3}\eta\nabla^2\bar{\phi}_t - \frac{1}{3}\nabla\bar{\phi} \cdot \nabla^3\bar{\phi}\right) - \frac{\epsilon^2}{45}\nabla^4\bar{\phi}_t = O(\epsilon^3, \alpha\epsilon^2, \alpha^2\epsilon) \end{aligned} \quad (6)$$

In principle the process could have been carried out to any order in α and ϵ . Neglecting the terms of order $\alpha\epsilon$ and ϵ^2 we reduce the above equations to a set of standard Boussinesq equation. The numerical solutions reported in section 5 always refer to these Boussinesq equations, and *not* to the full set (5) and (6).

For the radially symmetric case the Boussinesq equations inherent in (5) and (6) reduce to:

$$r\eta_t = -(r(1 + \alpha\eta)\bar{\phi}_r)_r \quad (7)$$

$$r(\bar{\phi}_t + \frac{1}{2}\alpha\bar{\phi}_r^2 + \eta) - \frac{1}{3}\epsilon(r\bar{\phi}_{rt})_r = 0 \quad (8)$$

where r is the distance from the axis of symmetry. Assuming only converging waves and $\frac{1}{r} = O(\alpha)$ we may derive the KdV equation :

$$\eta_t - \eta_r - \alpha\frac{3}{2}\eta\eta_r - \frac{1}{6}\epsilon\eta_{rrr} - \frac{1}{2r}\eta = 0 \quad (9)$$

which differ from the one employed by Miles (1977c) only due to scaling and direction of wave propagation. The set (7) and (8) is solved numerically in section 5.3, while the solutions of section 3 are checked by direct application of the perturbation scheme to (9), recognizing the factor before last term on the right hand side as being small and slowly varying.

Introducing a moving coordinate system (ζ, σ) :

$$\sigma = \frac{9}{2}\sqrt{\frac{\alpha}{2\epsilon}}\alpha t \quad \zeta = -3\sqrt{\frac{\alpha}{2\epsilon}}(r + t) \quad (10)$$

we obtain

$$\eta_\sigma + \eta\eta_\zeta + \frac{1}{2}\eta\zeta\zeta\zeta + \frac{1}{(2\sigma + 3\alpha\zeta)}\eta = 0 \quad (11)$$

Studying a wave system of finite extent we may adequately start the time integration at $t = t_1 = -r_1$ where r_1 defines the initial position of the system. If r_1 is sufficiently large the waves will then be confined to an interval with $|\alpha\zeta| \ll |\sigma|$ also for a period of the following time evolution. We are then led to ignore the ζ -term in denominator of the last term of (11) and arrive at an equation similar to the one solved by Ko & Kuehl (1978).

2.2 The soliton solution

Any reasonable measure of the length of a soliton is inversely proportional to the square root of the amplitude. Describing a plane soliton we thus set ϵ equal to α and write:

$$\eta = Y(\chi, \alpha) \quad \bar{\phi} = B\alpha^{-1}\Phi(\chi, \alpha) \quad (12)$$

where the linear phase function is defined as $\chi = k(\vec{n} \cdot \vec{r} - ct)$ in which \vec{n} is the unit vector in the direction of wave advance. The exact solution can be expressed through power series in α according to:

$$\left. \begin{aligned} Y &= Y_0 + \gamma_1\alpha Y_0^2 + \dots \\ \Phi_\chi &= Y_0 + \kappa_1\alpha Y_0^2 + \dots \\ k &= \frac{\sqrt{3\alpha}}{2}(1 + k_1\alpha + \dots) \\ c &= 1 + \frac{1}{2}\alpha + c_2\alpha^2 + \dots \\ B &= \frac{\alpha}{k} \end{aligned} \right\} \quad (13)$$

where $Y_0 = \text{sech}^2$ and α is explicitly defined by demanding the coefficient before Y_0 in the expansion for Y to equal 1. This gives a slightly different expansion parameter from those used by Laitone (1960) and Longuet-Higgins & Fenton (1974). The remaining coefficients, that are written out in (13), can be found by substitution into (5) and (6). Retaining only terms of order 1 and α we determine all numbers explicitly given in (13). In addition we obtain the relation:

$$\gamma_1 = 1 + \kappa_1 \quad (14)$$

Thus, this equation is inherited by any consistent weakly nonlinear and dispersive shallow water theory. This point will prove essential in the subsequent sections. Keeping also terms of order α^2 we may calculate also $\gamma_1, \kappa_1, k_1, c_1$ and b_1 . By introduction of terms of even higher order in (5) and (6) the expansion (13) could be carried still further, even though this would certainly be an impractical strategy for determining higher order solutions, let alone solitons of nearly extremal height. In the following sections we explicitly need only the leading terms of the expansion, but will still refer to Y and Φ as giving the exact solitary wave solution that in principle can be obtained from a generalized version of (5) and (6). According to Miles (1980) the question of convergence of such expansions is still somewhat open, but this will probably be of no consequence in the present context. A brief summary as to when and by whom the different terms of the expansion (13) were first reported is found in Witting (1975).

3 Perturbation solutions for slow variation and ray equation

The scaling given in (1) is particularly suited for development of long wave equations and perturbation solutions for waves of permanent form. However, it has now served its purpose and we introduce a different scaling using h_0^* as a measure of length for both horizontal and vertical coordinates. The new dimensionless variables read:

$$\left. \begin{aligned} x^* &= h_0^*x & y^* &= h_0^*y & t^* &= h_0^*(gh_0^*)^{-\frac{1}{2}}t \\ \eta^* &= h_0^*\eta & \phi^* &= h_0^*(gh_0^*)^{\frac{1}{2}}\phi & z^* &= h_0^*z \end{aligned} \right\} \quad (15)$$

We note that the amplitude factor α is no longer extracted from the surface elevation and velocity potential. Since the previous scaling (1) is never to reappear herein the same identifiers are used for the new dimensionless variables.

We will be dealing with wave patterns consisting of a single, nearly soliton shaped, crest as the primary wave field and, eventually, a secondary, or residual, system of diffracted waves. Whenever possible the x -axis will be aligned parallel to main direction of wave advance for the primary wave and the field variables evaluated at the crest peak will be marked by the superscript (m) .

3.1 Simple ray theory

For almost soliton shaped crests it exist an approximate theory analogous to wave kinetics for wave trains. The basic assumptions are similar: slow variation of topography and wave characteristics like amplitude and orientation. Ray equations for solitary waves have previously been reported by Miles (1977c), Reutov (1976), Kulikovskii & Reutov (1980) and Grimshaw (1971).

We formulate the equations in terms of the horizontal cartesian coordinates, x and y , rather than a curvilinear system adopted to the crest. The basis of the ray theory for solitons is the relation between the energy density measured pr. length of the crest, E , and the propagation speed, $c^{(m)}$, through the common dependence on the non-dimensional amplitude $A^{(m)}$, defined as the ratio between the crest height and the depth. In subsequent sections this interpretation of $A^{(m)}$ will be correct only to the leading order in a multiple scale expansion, but this is of no consequence in the present context. The ray theory, as presented below, consider only the primary crest while disregarding any deviation from the perfect solitary shape. Hence, the superscript is kept only with respect to consistent notation with subsequent sections. An expression for the energy density can be written:

$$E = (A^{(m)})^{\frac{3}{2}} \left(\frac{8}{3\sqrt{3}} + O(A^{(m)}) \right) \quad (16)$$

while the corresponding expression for $c^{(m)}$ is found by replacing α by $A^{(m)}$ in (13). An explicit representation of the higher order term indicated above is given in section 4.4. We assume that the position of the crest can be appropriately described by:

$$x = x^{(m)}(y, t) \quad (17)$$

Provided the energy transport (pr. length of the crest) can be approximated by $c^{(m)}E$ and is directed normal to the crest, conservation of energy leads to:

$$\frac{\partial}{\partial t} \left(\frac{1}{\cos \theta^{(m)}} E \right) = - \frac{\partial}{\partial y} (c^{(m)} E \tan \theta^{(m)}) \quad (18)$$

where $\theta^{(m)}$ is the angle between the crest and the y -axis. In addition to the energy equation we have the kinematic relation:

$$\frac{\partial x^{(m)}}{\partial t} = \frac{c^{(m)}}{\cos \theta^{(m)}} \quad (19)$$

or by differentiation with respect to y :

$$\frac{\partial \tan \theta^{(m)}}{\partial t} = - \frac{\partial}{\partial y} \left\{ \frac{c^{(m)}}{\cos \theta^{(m)}} \right\} \quad (20)$$

Given the proper initial conditions, the equations (18) and (20) may be solved for the unknowns $A^{(m)}$ and $\theta^{(m)}$. For small $\theta^{(m)}$ and $A^{(m)}$, the equations simplify to:

$$\frac{\partial e}{\partial t} = -\frac{\partial}{\partial y}(e\theta^{(m)}) \quad (21)$$

$$\frac{\partial \theta^{(m)}}{\partial t} = -\frac{1}{2} \frac{\partial}{\partial y}(e^{\frac{2}{3}} + (\theta^{(m)})^2) \quad (22)$$

where $e \equiv (A^{(m)})^{\frac{3}{2}}$. This set is readily recasted into a characteristic form according to:

$$\frac{d}{dt}(\sqrt{A^{(m)}} + \frac{1}{\sqrt{3}}\theta^{(m)}) = 0 \quad \text{at } C^+ : \frac{dy}{dt} = \theta^{(m)} + \sqrt{\frac{A^{(m)}}{3}} \quad (23)$$

$$\frac{d}{dt}(\sqrt{A^{(m)}} - \frac{1}{\sqrt{3}}\theta^{(m)}) = 0 \quad \text{at } C^- : \frac{dy}{dt} = \theta^{(m)} - \sqrt{\frac{A^{(m)}}{3}} \quad (24)$$

The expressions differ from those given by, for instance, Miles (1977) due to differences in coordinate systems and scaling only. It is easily realized that solutions of (23) and (24) will develop shocks that are analogous to the shock-shocks discussed in Whitham (1974). According to Miles (1977c) we may regard the junction between a Mach stem and the incident wave as such a shock. This idea is applied also by Yue & Mei (1980) in their analysis of abnormal reflection of Stokes waves. The recognition of a shock as the triple point of a phase locked triad (see Miles (1977b)) immediately imply that the crest diffract at the shock to create the third member of the triad. However, for small jumps in θ (weak shocks) the amplitude of the diffracted wave becomes very small.

A solution of (23) and (24) is compared to a numerical solution of the Boussinesq equations in figure 3. Although there are fair agreement in some respects, there are also important features that the simple theory presented above fails to reproduce. The main object of the remaining sections are to explain these discrepancies and accordingly to improve on equations like (21) and (22).

3.2 Formulation of the perturbation expansion, kinematic equations

We assume that the variation rate of height and orientation of the principal crest can be quantified by the small parameter β , which lead to introduction of slow variables $(\hat{x}, \hat{y}, \hat{t}) = \beta(x, y, t)$. The calculations are intimately related to those of Grimshaw (1970,71) and Ko & Kuehl (1979), but inherit several important modifications. As compared to that of Grimshaw the present perturbation scheme is simpler in the sense of not including variable depth or a strong mean current, but will on the other hand be advanced one order further in β . We will also introduce additional features in the expansion that are necessary to derive transport equations of higher order in β . These modifications also simplifies the description of the $O(\beta)$ wave field that is not explicitly reported by Grimshaw. For the axisymmetric case Ko & Kuehl do give the $O(\beta)$ contributions to the wave field. In addition to the limitations already inherent in their KdV equation (see: end of sec. 2.1) their perturbation scheme does not allow for spatial variation of amplitude. Consequently, as shown in section 3.6,

their solution will not be uniformly valid, but must be regarded as an inner solution for the primary crest. To obtain a complete solution this internal “boundary layer” solution must be matched to an asymptotic solution for the far field.

A perturbed soliton-like crest is written:

$$\left. \begin{aligned} \eta &= AY(\chi, A) + \beta\hat{\eta}(\chi, \hat{x}, \hat{y}, \hat{t}) + O(\beta^2) \\ \bar{\phi} &= B\Phi(\chi, A) + \beta\hat{\phi}(\chi, \hat{x}, \hat{y}, \hat{t}) + O(\beta^2) \end{aligned} \right\} \quad (25)$$

The form-functions Y and Φ are as defined in (13) with α replaced by A , that is a function of the slow variables \hat{x} , \hat{y} and \hat{t} . In the subsequent calculation A itself will serve as the ordering parameter for nonlinearity and dispersion. Expressed strictly it is $\beta A^{-\frac{1}{2}}$, rather than β itself, which has to be small. Thus we must expect $\hat{\eta} = O(A^{\frac{1}{2}})$, as will follow from the perturbation scheme. The phase function χ , that represent the fast variation, is no longer linear. Hence, the wavenumber, \vec{k} , and phase speed, c defined by:

$$\vec{k} = \nabla\chi \quad kc = -\chi_t \quad k = |\vec{k}| \quad (26)$$

are functions of \hat{x} , \hat{y} and \hat{t} . We note that, in contrast to in Grimshaw (1970,71)¹ the slow variables enter the expressions for Y and Φ only implicitly through A . Explicit dependencies of the primary field on the slow variables will complicate the calculation, obscure the results and may even give rise to nonuniformities. Thus, such dependencies should be avoided if possible. The local wavenumber and phase speed have to fulfill the consistency relations:

$$\vec{k}_t + \hat{\nabla}(kc) = 0 \quad \hat{\nabla} \times \vec{k} = 0 \quad (27)$$

Naturally, the variation of the characteristics of the primary wave will produce deviations from the perfect soliton shape, as represented by $\hat{\eta}$ and $\hat{\phi}$. In addition nonlinear interactions between the principal, soliton like crest (AY , $B\Phi$) and the residual wave field will alter the overall wave celerity speed. Hence, again deviating from Grimshaw, we expand c and \vec{k} according to:

$$c = c_0 + \beta c_1 \quad \vec{k} = \vec{k}_0 + \beta \vec{k}_1 \quad (28)$$

where c_0 , k_0 relate to A as described in (13), and c_1 , \vec{k}_1 are functions of χ and the slow variables. Defining $\vec{n} \equiv \cos\theta\vec{i} + \sin\theta\vec{j}$ as the unit vector parallel to \vec{k}_0 and correspondingly $\vec{s} = \vec{i}_z \times \vec{n}$ we decompose the wave number correction according to $\vec{k}_1 = N\vec{n} + S\vec{s}$. Exploiting (27) we find that N drops out to order β whereas c_1 and S are at most linear functions of χ :

$$c_1 = c_1^{(1)}(\hat{x}, \hat{y}, \hat{t})\chi + c_1^{(0)}(\hat{x}, \hat{y}, \hat{t}) + O(\beta) \quad (29)$$

$$S = S^{(1)}(\hat{x}, \hat{y}, \hat{t})\chi + S^{(0)}(\hat{x}, \hat{y}, \hat{t}) + O(\beta) \quad (30)$$

Since both c_0 and $c_1^{(1)}$ inherit only slow variation the term βc_1 may become comparable to c_0 for large χ , thereby violating the uniformity of the expansion (28). This indicates that only local validity of the perturbation solution can be anticipated when $c_1^{(1)}$ is nonzero. On the other hand, the fast variation associated with χ must be expected to

¹Grimshaw, as well as Ko & Kuehl (1978), introduced a multiplicative factor, p , depending on slow variables, before the phase function in a quantity corresponding to Y_0 . In his case this probably present no problem because he do not explicitly give or discuss $\hat{\eta}$, $\hat{\phi}$.

vanish when $|\chi| \rightarrow \infty$. It turns out that we generally obtain a solution that is local in the slow variables, but still correct for large χ . We are now led to the kinematic relations:

$$\vec{k}_{0,\hat{t}} + c_f \vec{n} \cdot \hat{\nabla} \vec{k}_0 = -k_0^2 c_1^{(1)} + O(\beta) \quad (31)$$

$$\theta_{\hat{t}} + c_f \vec{n} \cdot \hat{\nabla} \theta = (c_0 - c_f) S^{(1)} + O(\beta) \quad (32)$$

The factor $c_f = (k_0 c_0)_A / k_{0,A}$ bears a formal resemblance to the group velocity for sinusoidal waves and occur in a similar fashion as far as the kinematic equations are concerned. However, the quantity $c_f = 1 + \frac{3}{2}A + O(A^2)$ does not give the energy celerity speed, which for solitons equals $c_0 = 1 + \frac{1}{2}A + O(A^2)$. Later, the two equations (31) and (32) will be supplied by a third equation that emerges from the solubility condition for $\hat{\eta}$ and $\hat{\phi}$. If $c_1^{(1)}$ and $S^{(1)}$ were not included in the calculation we would then have a set of three equations for the two unknowns A and θ , for which the existence of a solution is far from obvious in beforehand. This problem is not discussed by Grimshaw – a redefinition of the intrinsic phase speed, as given in (28), may be hidden in his wave/current interactions. However, we do find solutions having $S^{(1)} = c_1^{(1)} = 0$ for the two cases reported in section 3.5 and 3.6 respectively. The retainment of $c_1^{(1)}$ and $S^{(1)}$ do also reconcile the present approach to the one reported by Ko & Kuehl. Expressed in the present notation they essentially assumed a phase function of the form:

$$\chi = k(\hat{t})(r - r_0(t)) + R(\hat{t}) \quad (33)$$

where $r_{0,t}$ is slowly varying. From this expression we find:

$$k = k(\hat{t}) \quad c = r_{0,t} - \frac{\beta}{k^2}(k_{\hat{t}}\chi + kR_{\hat{t}} - k_{\hat{t}}R) \quad (34)$$

which is consistent with (29). We have also investigated the possibility of retaining a nonzero N , but have not found this advantageous.

At the peak of the primary wave only $c_1^{(0)}$ will contribute to the wave celerity speed. As an alternative to the introduction of $c_1^{(0)}$ we could have allowed A to be redefined to each order in β . To avoid ambiguity we must exclude such modifications that, according to (13), will appear as:

$$\hat{\eta} = \dots + A_1(\hat{x}, \hat{y}, \hat{t})(Y_0 + \frac{1}{2}\chi Y_{0,x}) + \dots \quad (35)$$

where βA_1 is the first order amplitude correction. According to the discussion in the preceding paragraphs we are left with some freedom concerning the spatial variation in A in relation to the factors $c_1^{(1)}$ and $S_1^{(1)}$. Apart from plane and axisymmetric cases a lateral (along primary crest) variation in A must be fully included. The normal variation do however seem less essential, as reflected by the procedure of Ko & Kuehl. Using the axisymmetric case as an example we may rewrite a solution with variable A by inserting $A = A^{(m)} + \beta A_{\hat{r}}^{(m)}(r - r^{(m)}) + O(\beta^2)$ into the primary solution and expand in powers of β . Denoting the new phasefunction $k^{(m)}(r - r^{(m)})$ by χ we find that the spatial variation of A to leading order correspond to the following contribution to the secondary wave field:

$$\hat{\eta} = \dots + \frac{A_{\hat{r}}^{(m)}}{k^{(m)}}(\chi Y_0 + \frac{1}{4}\chi^2 Y_{0,x}) + \dots \quad (36)$$

Contrary to that in (35) this term will have no implications for the the derivation of the higher order transport equations in section 4 because it is odd in χ .

The position of the primary peak is given by $\chi = 0$. If the surface is denoted by $x = x^{(m)}(y, t)$, as in section 3.1, the kinematic equation (20) still apply provided the value of $c^{(m)}$ is modified according to (28). For derivatives of a general function, f , we may then write:

$$f_{\hat{t}}^{(m)} = (f_{\hat{t}} + \frac{c}{\cos \theta} f_{\hat{x}})|_{\hat{x}=\hat{x}^{(m)}} \quad f_{\hat{y}}^{(m)} = (f_{\hat{y}} - \tan \theta f_{\hat{x}})|_{\hat{x}=\hat{x}^{(m)}} \quad (37)$$

3.3 The first order solution.

Generally we must expect that a residual system of diffracted waves is trailing the leading crest. Thus, we may impose that $\hat{\eta}$ and $\hat{\phi}$ vanish asymptotically upstream ($\chi \rightarrow \infty$), while allowing an infinite extension downstream for the first order wave field. Inserting (25), (26) and (28) into the rescaled versions of (5) and (6) and integrating the continuity equation with respect to χ we find that the leading balance is automatically fulfilled through the definition of the soliton solution, while we to first order in β obtain:

$$-c_0 \hat{\eta} + k_0 \hat{\phi}_\chi = c_1^{(0)} A Y + c_1^{(1)} A \int_{\infty}^{\chi} \chi Y_\chi d\chi \quad (38)$$

$$-k_0^{-1} A_{\hat{t}} \int_{\infty}^{\chi} Y d\chi - k_0^{-1} (2 \hat{\nabla} B \cdot \vec{k}_0 + B \hat{\nabla} \cdot \vec{k}_0) \Phi + S_1$$

$$-\hat{\eta} + c_0 k_0 \hat{\phi}_\chi = -(c_1^{(0)} + c_1^{(1)} \chi) k_0 B \Phi_\chi + B_{\hat{t}} \Phi + S_2 \quad (39)$$

where $S_1, S_2 = O(A^{\frac{3}{2}})$. The set (38) and (39) can be ruled by two alternative dominant balances, corresponding to different representations of the secondary wave field. In any case it turns out that

$$\hat{\eta} = O(A^{\frac{1}{2}}) \quad \theta_s = O(A) \quad c_1^{(0)}, c_1^{(1)} = O(A^{\frac{1}{2}}) \quad (40)$$

We may summarize the two choices as follows:

(i) $-\hat{\eta} + k_0 \hat{\phi}_\chi = O(A^{\frac{1}{2}})$

The two left hand sides become equal to order $A^{\frac{1}{2}}$. A solution for $\hat{\eta}$ and $\hat{\phi}$ is thus possible only if:

$$A_{\hat{t}}, \vec{n} \cdot \hat{\nabla} A = O(A) \quad T \equiv B_{\hat{t}} + k_0^{-1} (A_{\hat{t}} + 2 \hat{\nabla} B \cdot \vec{k}_0 + B \hat{\nabla} \cdot \vec{k}_0) = O(A^{\frac{3}{2}}) \quad (41)$$

To leading order (31) now imply $A_{\hat{t}} + \vec{n} \cdot \hat{\nabla} A = O(A^2)$ which is consistent with (41). In this case all $O(A^{\frac{3}{2}})$ terms in S_1, S_2 become significant.

(ii) $-\hat{\eta} + k_0 \hat{\phi}_\chi = O(A^{\frac{3}{2}})$

As compared to the preceding option the variation of A becomes one order higher in A , according to $A_{\hat{t}}, \vec{n} \cdot \hat{\nabla} A = O(A^2)$. Consequently, the variation of A and k_0 can not contain the $O(\beta)$ modifications of the wave profile and a term like (36) is bound to appear. The solution for $\hat{\eta}$ and $\hat{\phi}$ is again determined through the $O(A^{\frac{3}{2}})$ balance of (38) and (39). However, this time we may retain only the terms in S_1 and S_2 that contain $\hat{\eta}$ or $\hat{\phi}$.

Only the balance (i) enable compact and uniform solutions, while (ii) yields much simpler calculations. For the derivations below we assume the behaviour (i). The alternative choice would involve the same main steps and lead to identical final equations (45) through (49). Some of the terms that are retained in these equations would, however, become insignificant.

Invoking (41) we find the following expressions for S_1 and S_2 :

$$\left. \begin{aligned} S_1 &= -Ak_0 Y \hat{\phi}_\chi - Bk_0 \Phi_\chi \hat{\eta} - k_0^{-1} \nabla \cdot (AB \vec{k}_0) \int_\infty^\chi Y \Phi_\chi d\chi \\ &\quad - A \vec{n} \cdot \hat{\nabla} B \Phi Y - k_0^{-1} A A_{\hat{t}} \int_\infty^\chi Y_A d\chi - 2B \vec{n} \cdot \hat{\nabla} A \Phi_A + O(A^{\frac{5}{2}}) \\ S_2 &= Bk_0^2 \Phi_\chi \hat{\phi}_\chi + B \vec{k}_0 \cdot \hat{\nabla} B \Phi \Phi_\chi + B A_{\hat{t}} \Phi_A \\ &\quad + \frac{1}{3} k_0^3 \hat{\phi}_{\chi\chi\chi} - \frac{1}{3} \left((k_0^2 B)_{\hat{t}} - 2k_0 \vec{k}_0 \cdot \hat{\nabla} B - k_0 B \hat{\nabla} \cdot \vec{k}_0 \right) \Phi_{\chi\chi} + O(A^{\frac{5}{2}}) \end{aligned} \right\} \quad (42)$$

We note that, to the present order in A , terms of higher order than α and ϵ in (5) and (6) contribute only implicitly through Φ and Y . Using the dominant balance of (39) $\hat{\phi}$ is easily eliminated between (39) and (38). Utilizing the kinematic equations (31) and (32) we may recast the resulting equation for $\hat{\eta}$ into the form:

$$\begin{aligned} \frac{1}{4} \hat{\eta}_{0,\chi\chi} + (3Y_0 - 1) \hat{\eta}_0 &= \left(\frac{1}{2\sqrt{3}} A^{-\frac{1}{2}} A_{\hat{t}} - A^{-1} T - c_1^{(1)} \right) \Phi_0 + 2(c_1^{(0)} + c_1^{(1)} \chi) Y_0 \\ &\quad + \frac{5}{4\sqrt{3}} A^{-\frac{1}{2}} A_{\hat{t}} Y_{0,\chi} + O(A^{\frac{3}{2}}) \end{aligned} \quad (43)$$

where $\Phi_0 \equiv \int_\infty^\chi Y_0 d\chi = 1 - \tan \chi$. We note that Φ_0 , Y_0 and $Y_{0,\chi}$ are linearly independent functions of χ and that terms involving κ_1 has canceled during the calculations. One solution of the homogeneous counterpart of the equation is $Y_{0,\chi}$. Then, the complementary part of the full solution of (43) is readily found:

$$\begin{aligned} \hat{\eta}_0 &= D_1(\hat{x}, \hat{y}, \hat{t}) Y_{0,\chi} + D_2(\hat{x}, \hat{y}, \hat{t}) G(\chi) - \left(\frac{1}{2\sqrt{3}} A^{-\frac{1}{2}} A_{\hat{t}} - A^{-1} T - c_1^{(1)} \right) \Phi_0 \\ &\quad + (2c_1^{(0)} - 3 \left(\frac{1}{2\sqrt{3}} A^{-\frac{1}{2}} A_{\hat{t}} - A^{-1} T - c_1^{(1)} \right)) (Y_0 + \frac{1}{2} \chi Y_{0,\chi}) \\ &\quad + \frac{5}{4} \left(\frac{1}{2\sqrt{3}} A^{-\frac{1}{2}} A_{\hat{t}} + A^{-1} T \right) R(\chi) \\ &\quad + 2c_1^{(1)} (\chi Y_0 + \frac{1}{4} \chi^2 Y_{0,\chi}) + O(A^{\frac{3}{2}}) \end{aligned} \quad (44)$$

where D_1 and D_2 are constants of integration, G is a homogeneous solution independent of $Y_{0,\chi}$ and R is a particular solution corresponding to replacing the right hand side of (43) with $Y_{0,\chi}$. The calculation of R and G is straightforward and the essential results in the present context are that $G \sim \exp |\chi|$, $R \sim \exp 2|\chi|$ as $|\chi| \rightarrow \infty$. Hence, D_2 as well as the coefficient before R in (44) have to be zero, which determine T and finally imply (45) given below. According to the discussion below equation (28) we must discard also the term on the second line of (44), thereby assigning a value to c_1 . Generally, any terms involving powers of χ , instead of neatly behaved combinations of exponentials, look suspicious and should preferably be reinterpreted or removed by an improved construction of the perturbation scheme. Also the last term of (44) contain potential factors of χ . However, this term, that is of the form given in (36), can be removed only by finding solutions for A and θ giving zero $c_1^{(1)}$. Now then, the term $D_1 Y_{0,\chi}$ is easily seen to correspond to a nonuniform representation of a redefined phasefunction given by $\chi \rightarrow \chi + \beta D_1$. This redefinition will not alter the profile of the principal crest to order β and correspond to $O(\beta^2)$ modifications in \vec{k}

and c that preferably should enter the solution through higher order corrections to the transport equations. The fact that Ko & Kuehl find a distinct value for D_1 from a higher order solubility condition is probably due to the absence of expansions, like (28), for c and k in their perturbation scheme. Clearly, in a consistent and compact expansion we can put D_1 to zero. In addition we may note that this term will not contribute anyway to the energy integrals in section 4. Using the dominant balance inherent in the kinematic equations (31) and (32) we can rewrite the requirement of vanishing coefficient before R in (44) according to:

$$(A^{\frac{3}{2}})_{\hat{t}} + c_0 \hat{\nabla} \cdot (\bar{n} A^{\frac{3}{2}}) = O(A^{\frac{7}{2}}) \quad (45)$$

The equation is easily brought into standard conservative form, but this is really inadequate since it does not, by itself, express local energy conservation. On the other hand, applying (37) and (20) we find that (45) is consistent with (18) and thereby imply energy conservation in an integrated sense. The error term in (45) may seem to be of surprisingly high order in A . However, according to the kinematic equations $\nabla \cdot \bar{n} = O(A)$ and leading order of (45) simply states $A_{\hat{t}} + \hat{\nabla} \cdot (\bar{n} A) = O(A^2)$. An $O(A^{\frac{5}{2}})$ correction to the "energy density" $A^{\frac{3}{2}}$ in (45) will thus correspond to an $O(A^{\frac{7}{2}})$ modification of the right hand side. Combining (45) and (31) we find expressions for the phase speed corrections:

$$c_1^{(1)} = \frac{1}{\sqrt{3}} A^{-\frac{1}{2}} (-\bar{n} \cdot \hat{\nabla} A + \frac{2}{3} \theta_{\hat{s}}) + O(A^{\frac{3}{2}}) \quad (46)$$

$$c_1^{(0)} = \frac{3}{2} \left(\frac{1}{\sqrt{3}} A^{-\frac{1}{2}} A_{\hat{t}} - c_1^{(1)} \right) + O(A^{\frac{3}{2}}) = -\frac{1}{\sqrt{3}} A^{-\frac{1}{2}} \theta_{\hat{s}} + O(A^{\frac{3}{2}}) \quad (47)$$

where the superscript \hat{s} denotes derivation along lines of constant phase according to $\theta_{\hat{s}} \equiv \bar{s} \cdot \hat{\nabla} \theta$. We note that the correction to the phase speed at the peak is proportional to $\theta_{\hat{s}}^{(m)}$ which is the curvature of the principal crest. Substituting the solution for $\hat{\eta}$ into (39) we obtain the first order wave field:

$$\hat{\eta} = \frac{2}{3\sqrt{3}} A^{-\frac{1}{2}} \theta_{\hat{s}} \Phi_0 + 2c_1^{(1)} (\chi Y_0 + \frac{1}{4} \chi^2 Y_{0,x}) + O(A^{\frac{3}{2}}) \quad (48)$$

$$\hat{\phi} = k_0^{-1} c_1^{(1)} (\chi \Phi_0 + \frac{1}{2} \chi^2 Y_0) + O(A) \quad (49)$$

From the above expression for $\hat{\phi}$ and (25) we obtain a nonzero cross ray velocity, defined as the component along \bar{s} , that becomes important in section 4. This velocity component is induced by the lateral pressure gradients associated with the non-uniformity of the primary wave.

Equation (47) and (48) imply that a converging, or focusing, crest ($\theta_{\hat{s}} < 0$) has an increased propagation velocity and is followed by a surface elevation, whereas a diverging wave is retarded and followed by a trough. As a consequence, the modification $c_1^{(0)}$ to the wave speed will tend to straighten a crest that inherits alternating focusing and defocusing regions.

3.4 Uniformity and diffracted wave field

Behind the primary wave ($\chi \rightarrow -\infty$) Y and Φ_χ decay exponentially, whereas $\Phi_0 \rightarrow -2$. Consequently the downstream wave field does not vanish, but is defined through:

$$\left. \begin{aligned} \eta_{-\infty} &= 2\beta\left(\frac{1}{\sqrt{3}}A^{-\frac{1}{2}}A_{\hat{t}} - c_1^{(1)}\right) = -\frac{4\beta}{3\sqrt{3}}A^{-\frac{1}{2}}\theta_{\hat{s}} \\ \phi_{-\infty} &= -2B - 2\beta\frac{c_1^{(1)}}{k_0}\chi \\ \vec{v}_{-\infty} &= -2\beta(\hat{\nabla}B + c_1^{(1)}\vec{n}) = \frac{-\beta}{\sqrt{3}}A^{-\frac{1}{2}}\left(\frac{4}{3}\theta_{\hat{s}}\vec{n} + 2A_{\hat{s}}\vec{s}\right) \end{aligned} \right\} \quad (50)$$

where $\vec{v}_{-\infty}$ is the particle velocity and relative errors of order A, β is implicit throughout. If the solution of the previous subsection is a uniform solution the above wave field itself has to be a valid solution of the hydrodynamic equations. Otherwise 50 will be correct only for $x = x^{(m)}$ (immediately behind the primary crest). We note that the amplitude of the limiting wave field is proportional to $\beta A^{\frac{1}{2}} \ll A$ and that all spatial variation of the physical quantities appear through the slow variables only. Therefore, $\eta_{-\infty}$ and $\vec{v}_{-\infty}$ should fulfill the linear hydrostatic equations:

$$\vec{v}_{-\infty,t} + \nabla\eta_{-\infty} = 0 \quad \eta_{-\infty,t} = -\nabla \cdot \vec{v}_{-\infty} \quad (51)$$

to the leading order in A and β . It is easily deduced that any solution with $S^{(1)} = c_1^{(1)} = 0$ meet these requirements. Still, as experienced for the axisymmetric case in section 3.6, there may not be any such solution that is strictly uniform. On the other hand, for the case in section 3.5 we find uniform solutions also for a restricted class of nonzero $S^{(1)}, c_1^{(1)} = 0$. Even if only locally valid, the perturbation solution provides boundary values for the far field solution that is governed by linear hydrostatic theory. The matching values for η and \vec{v} is obtained simply by inserting $x = x^{(m)}$ in the rightmost expressions in (50).

3.5 Perturbations on straight crests

We assume small perturbations on a uniform crest aligned parallel to the y -axis. Guided by (23) and (24) we introduce the rescaled variables:

$$\left. \begin{aligned} \tilde{\xi} &= A_0^{-\frac{1}{2}}(\hat{x} - c_0(A_0)\hat{t}) & \tilde{t} &= A_0^{\frac{1}{2}}\hat{t} \\ A &= A_0(1 + \nu a) & \theta &= \nu A_0^{\frac{1}{2}}\psi \end{aligned} \right\} \quad (52)$$

where A_0 is the reference amplitude for the undisturbed carrier wave and the small parameter ν is a measure of the magnitude of the perturbation. The scaling of $\tilde{\xi}$, that essentially correspond to $x - x^{(m)}$, indicates a larger rate of change in a and ψ normal to the crest as compared to the lateral direction. Inserting (52) in (32), (45) and (46) and retaining only linear terms in ν we obtain to the leading order in A_0 :

$$\left. \begin{aligned} \text{(a): } \psi_{\tilde{t}} + \psi_{\tilde{\xi}} &= -\frac{S^{(1)}}{\nu} & \text{(b): } a_{\tilde{t}} + \frac{2}{3}\psi_{\tilde{y}} &= 0 \\ \text{(c): } a_{\tilde{t}} + a_{\tilde{\xi}} &= -\frac{\sqrt{3}}{\nu}c_1^{(1)} \end{aligned} \right\} \quad (53)$$

To the same level of approximation the kinematic equation (20) gives:

$$\psi_{\tilde{t}}(0, \hat{y}, \tilde{t}) = -\frac{1}{2}a_{\tilde{y}}(0, \hat{y}, \tilde{t}) \quad (54)$$

If we choose $S^{(1)} = 0$ the combination of (53ab) and (54) leads to:

$$\psi = \psi_+(\hat{y} + \frac{1}{\sqrt{3}}(\tilde{\xi} - \tilde{t})) + \psi_-(\hat{y} - \frac{1}{\sqrt{3}}(\tilde{\xi} - \tilde{t})) \quad (55)$$

while a in addition to functions of the composite variables $\hat{y} \pm \frac{1}{\sqrt{3}}(\tilde{\xi} - \tilde{t})$ also includes a general function of $\tilde{\xi}$. Setting this constant of integration to zero we find $c_1^{(1)} = 0$ and transformation back to \hat{x} , \hat{y} yields:

$$a = a_+(\hat{y} + (3A_0)^{-\frac{1}{2}}\hat{x} - \Omega\hat{t}) + a_-(\hat{y} - (3A_0)^{-\frac{1}{2}}\hat{x} + \Omega\hat{t}) \quad (56)$$

where $\Omega = (3A_0)^{-\frac{1}{2}} + \frac{1}{2}(3A_0)^{\frac{1}{2}} + O(A_0^{\frac{3}{2}})$. Applying 50 we find

$$\eta_{-\infty} = -\frac{4\beta\nu}{3\sqrt{3}}\psi_{\hat{y}}(1 + O(A, \beta, \nu)) \quad (57)$$

$$\vec{v}_{-\infty} = \frac{\beta\nu}{\sqrt{3}}(-\frac{4}{3}\psi_{\hat{y}}\vec{i} + 2A_0^{\frac{1}{2}}a_{\hat{y}}\vec{j})(1 + O(A, \beta, \nu)) \quad (58)$$

and recognize two families of diffracted waves. The two systems have phase lines aligned at angles $\pm\sqrt{3A_0}$ relative to the primary crest and are linked to perturbations propagating along the C^\pm characteristics in (23) and (24) respectively. The solution (56) corresponds to straight crested waves with wavenumber $\vec{K} = \pm(3A_0)^{-\frac{1}{2}}\vec{i} + \vec{j}$ and frequency $^2 \pm\Omega$ that satisfy the relation:

$$\Omega^2 = K^2(1 + O(A_0^2)) \quad (59)$$

Hence, the diffracted wave system is a solution of the linear hydrostatic equations.

As one alternative to putting $S^{(1)}$ equal to zero we could have prescribed that a and ψ in (53) are independent of $\tilde{\xi}$ in line with alternative (ii) on page 11. We would then get nonzero $c_1^{(1)}$ and $S^{(1)}$ as functions of time. The local solution (finite χ) inherent in (25), (48) and (49) would be valid, but we would not obtain a correct residual wave field from (50). In this case the matching to the far field is easily performed, due to the simplicity of the crest modulations, and we reproduce the solution outlined above.

From (53) it is immediately realized that that the residual field can be correctly calculated by (50) whenever $c_{1,\hat{y}}^{(1)} = S_{\hat{y}}^{(1)} = 0$. Hence, any such choice will also correspond to perturbation solutions of uniform validity.

3.6 The axisymmetric case

Sufficiently far away from the point of symmetry (large r) we may regard focusing or defocusing of solitary waves as a special case of the slow variation theory described previously. Confining ourselves to converging waves we may identify \vec{n} as $-\vec{i}_r$, the inward radial unit vector, and set $A = A(\hat{r}, \hat{t})$. While equation (32) loses its significance (31) simplifies to:

$$A_{\hat{t}} - c_f A_{\hat{r}} = -\sqrt{3}A^{\frac{3}{2}}c_1^{(1)} + O(A^3) \quad (60)$$

²The definitions of \vec{K} and Ω are arbitrary with respect to a common multiplicative constant. Thus, the occurrence of inverse square roots of A_0 does not correspond to short waves.

From the “energy” equation, (45), we find:

$$\hat{r}(A^{\frac{3}{2}})_{\hat{t}} - c_0(\hat{r}A^{\frac{3}{2}})_{\hat{r}} = O(A^{\frac{7}{2}}) \quad (61)$$

that directly express:

$$rA^{\frac{3}{2}} = \text{const.} + O(rA^{\frac{5}{2}}) \quad \text{at} \quad r(t) : r_{\hat{t}} = -c_0 \quad (62)$$

The expression for $c_1^{(1)}$ becomes:³

$$c_1^{(1)} = -\frac{1}{\sqrt{3A}}\left(\frac{2}{3\hat{r}} - A_{\hat{r}}\right) + O(A^{\frac{3}{2}}) \quad (63)$$

which together with either one of (61) or (60) implies the other. This time the uniformity of the solutions require that the far-field solution attains the form:

$$\eta_{-\infty} = \frac{F(r+t)}{\sqrt{r}}\left(1 + O\left(\frac{1}{r}\right)\right) \quad (64)$$

where F is any well behaved function. An $A(\hat{r}, \hat{t})$ that both lead to such an expression for $\chi \rightarrow -\infty$ and fulfill (61) within an relative error $O(r^{-2})$ is given by:

$$A = \frac{2(\hat{r} + \hat{t} + \hat{t}_0)}{3\hat{r}} \quad (65)$$

where \hat{t}_0 is a constant of integration which approximately yields $A(r^{(m)}, t) = A^{(m)}$. However, for $r \gg r^{(m)}$ the quantity A defined by (65) is no longer small and one of the basic assumptions is violated. Since the large values of A do not correspond to large waveheights we might possibly have circumvented this problem by a modified perturbation scheme. However, we prefer to regard the use of (65) as a “built-in” match and denote the corresponding solution as being unified. Equation (65) also implies that A change sign at a distance $\Delta r = \frac{3}{2}r^{(m)}A^{(m)}$ ahead of the peak position. Consequently, the described solution is singular at $r = r^{(m)} - \Delta r$ and becomes undefined beyond this point. However, this irregularity is of minor importance as long as Δr is much larger than the length of the primary wave ($\Delta r \gg (A^{(m)})^{-\frac{1}{2}}$). Thus, as long as the assumption of slow variation is properly fulfilled we may neglect the singularity. A removal of the singularity through inclusion of higher order terms has not been attempted.

Inserting the expression (65) for A in (63) we find that $c_1^{(1)}$ vanish to leading order in A . Equation (48) now imply:

$$\hat{\eta} = -\frac{2}{3\hat{r}\sqrt{3A}}\Phi_0 \quad (66)$$

which demonstrates the existence of a tail to the primary crest, that slowly decays for increasing r . To leading order the phasefunction becomes:

$$\chi = \int_{r^{(m)}}^r kdr = kr - k^{(m)}r^{(m)} - \frac{\gamma}{\sqrt{2}} \ln \sqrt{\frac{r}{\gamma}}(1 + \sqrt{2}k) \quad (67)$$

³The curvature is $-1/\hat{r}$ due to the clockwise orientation of \vec{s} .

where $\gamma = r^{(m)}(1 - \frac{3}{2}A^{(m)})$.

The assumption of a radially constant A correspond to $A \equiv A^{(m)}(\hat{t})$ where $A^{(m)}$ can be found from (62) substituted $r = r^{(m)}$. The simple solution (67) is then replaced by an expression of somewhat more awkward appearance:

$$\hat{\eta} = -\frac{2}{3r\sqrt{3A^{(m)}}}(\Phi_0 + 2(\chi Y_0 + \frac{1}{4}\chi^2 Y_{0,x})) \quad (68)$$

that is similar in form to the solution of Ko & Kuehl. On the other hand, the phase function now becomes trivial:

$$\chi = k^{(m)}(r - r^{(m)}) \quad (69)$$

Through application of (36) it is straightforward to demonstrate consistency between (66), (67) and (68), (69) for finite χ . However, the latter solution becomes invalid for large r ($\chi \rightarrow -\infty$). Apart from two extra terms the corresponding expression of Ko & Kuehl can be rewritten as (68). In addition to the term $D_1 Y_{0,\chi}$ (see eq. (44) and the following discussion) the solution of Ko & Kuehl also contains a term of type (35) corresponding to a redefinition of the amplitude: $A_1 = -4/(3r^{(m)}\sqrt{3A^{(m)}})$. When this amplitude modification is taken into account we find that results of Ko & Kuehl also become consistent with $c_1^{(0)}$ as given in (47).

4 Application of conservation laws.

The $O(\beta)$ correction to the energy transport equation can be found by going to higher order in the perturbation scheme. However, to leading order the energy equation can be deduced by a direct energy balance argument applied to the primary wave field, as is indicated in section 3.1. Correspondingly, similar arguments applied to the corrected wave field, calculated in the preceding section, will result in a higher order energy equation. As compared to advancing the perturbation scheme this will constitute a simpler and altogether more illustrative approach.

4.1 Integrated conservation laws

A control volume for mass, momentum and energy balance is depicted in figure 1. Using the notations implicit in the figure and letting $y_1 - y_0 \rightarrow 0$ we obtain the integrated conservation law:

$$\beta \mathcal{E}_t + \tilde{\mathcal{E}}_t = -\beta \mathcal{F}_y - \tilde{\mathcal{F}}_y + \tilde{f}^{(x)} \quad (70)$$

where \mathcal{E} and \mathcal{F} are the integrated (parallel to x) density and flux density in the y -direction, respectively, owing to the primary wave field and its couplings with higher order corrections in β . Due to the decay of the $O(\beta^0)$ field, the contributions to these quantities are confined to within the extent of the leading principal crest. The quantities $\tilde{\mathcal{E}}$ and $\tilde{\mathcal{F}}$ are the corresponding density and flux density belonging to the higher order corrections alone, which must be found by integrating the local densities, respectively $\tilde{\epsilon}$ and $\tilde{f}^{(y)}$, over the total cross-sections of the control volume. Finally, the last term $\tilde{f}^{(x)}$ is simply the x component of the flux density in the diffracted wave field. The mixture of slow and fast variables in (70) reflects the magnitude of the

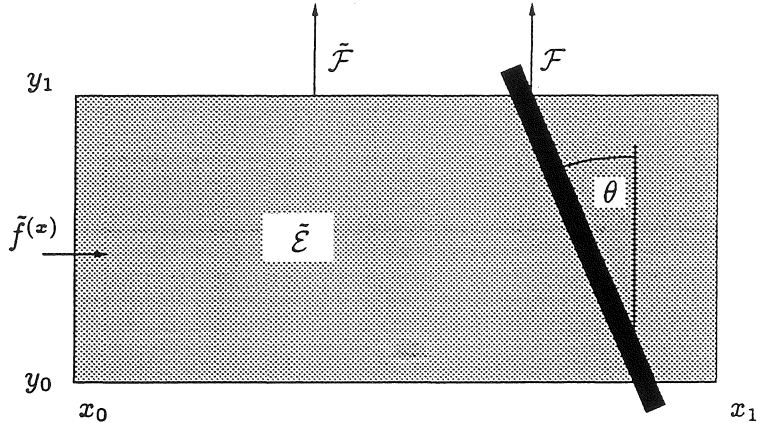


Figure 1: Control volume for energy account. The volume corresponds to the shaded region, while the fat solid line indicates the primary wave.

relative rates of changes in time and space. The fast changes associated with the tilde-quantities in (70) stem from the changes of the length of the trailing wavefield defined as $x^{(m)} - x_0$. Assuming the length $x_1 - x_0$ to be short relative to the long spatial scale we then obtain from geometrical considerations:

$$\tilde{\mathcal{E}}_t = \frac{c^{(m)}}{\cos \theta^{(m)}} \tilde{\varepsilon} (1 + O(\beta)) \quad \tilde{\mathcal{F}}_y = -\tan \theta^{(m)} \tilde{f}^{(y)} (1 + O(\beta)) \quad (71)$$

where the local densities is to be calculated at the position of the ridge, $x = x^{(m)}$.

If the conserved quantities are volume, defined as increase from undisturbed state, or momentum we may write $\tilde{\varepsilon} = \beta \hat{\varepsilon}$ and $\tilde{f}^{(x),(y)} = \beta \hat{f}^{(x),(y)}$ where $\hat{\varepsilon}$, $\hat{f}^{(x)}$, and $\hat{f}^{(y)}$ are of order β^0 . From (70) we may then obtain:

$$\mathcal{E}_t = -\mathcal{F}_y + \tan \theta^{(m)} \hat{f}^{(y)} - \frac{c^{(m)}}{\cos \theta^{(m)}} \hat{\varepsilon} + \hat{f}^{(x)} + O(\beta) \quad (72)$$

We note that the $O(\beta)$ wave field enters the dominant balance of the conservation equations. Knowing the primary field, we may then calculate the residual wavefield behind the crest, in analogy with the calculation of the reflections from a plane soliton over a sloping bottom reported by, for instance, Knickerbocker and Newell (1985). However, neither the higher order field within the primary crest, which is important for the energy account below, nor any higher order transport equations can be determined through the integrated conservation law for volume and momentum. In the present context (72) is thus useful primarily as a test for results calculated in section 3.

Applying (72) to volume and both components of horizontal momentum and combining the resulting equations with (45) and (20) we reproduce the expressions in (50) for the surface elevation and velocity immediately behind the principal crest. In addition we obtain the new relation:

$$\vec{n} \cdot \vec{v}_{-\infty} - \eta_{-\infty} = -\frac{3}{2} A^{(m)} \eta_{-\infty} (1 + O(A)) \quad (73)$$

which is consistent with the plane diffracted wave of section 3.5.

4.2 The higher order energy equation.

The energy density behind the leading crest is of order β^2 . We may thus write $\bar{\varepsilon} = \beta^2 \hat{\varepsilon}$ and $\bar{f}^{(x),(y)} = \beta^2 \hat{f}^{(x),(y)}$. Further we invoke the partition: $\mathcal{F} = \mathcal{F}_0 + \beta \mathcal{F}_1$, $\mathcal{E} = \mathcal{E}_0 + \beta \mathcal{E}_1$. The first order parts are associated with products between $O(1)$ and $O(\beta)$ field variables and variations of A , \vec{k} and c across the crest. However, the latter contribution will turn out to be zero. The conservation law may now be recasted into the ordered form:

$$\mathcal{E}_{0,\hat{t}} + \beta \mathcal{E}_{1,\hat{t}} = -\mathcal{F}_{0,\hat{y}} - \beta \mathcal{F}_{1,\hat{y}} - \beta \mathcal{D} + O(\beta^2) \quad (74)$$

$$\mathcal{D} = -(f^{(x)} + \tan \theta^{(m)} \hat{f}^{(y)} - \frac{c^{(m)}}{\cos \theta^{(m)}} \hat{\varepsilon}) + O(\beta^2) \quad (75)$$

where \mathcal{D} can be interpreted as the energy leak due to the diffracted wave field. Neglecting terms proportional to β in this equation we may now reproduce the zeroth order energy transport equation (18). Retaining terms of order β and substituting the wavefield given through (25), (48) and (49) into the integrals implicit in (74) we obtain a higher order transport equation.

The integrands in the expressions for \mathcal{E}_i and \mathcal{F}_i decays exponentially at the outskirts of the primary wave. Over the significant integration interval we may thus write: $\chi = k^{(m)} \cos \theta^{(m)}(x - x^{(m)}) + O(\beta)$, where the superscript m still refers to the crest peak. In terms of order β we may thus invoke a linear relation between χ and x without further argumentation. Generally we may write:

$$\begin{aligned} \int_{-\infty}^{\infty} G(\chi, \hat{x}) dx &= \int_{-\infty}^{\infty} \frac{G(\chi, \hat{x}^{(m)})}{k^{(m)} \cos \theta^{(m)}} d\chi \\ &+ \beta \int_{-\infty}^{\infty} \frac{\partial}{\partial \hat{x}} \left(\frac{G}{k \cos \theta} \right)^{(m)} \frac{\chi}{k^{(m)} \cos \theta^{(m)}} d\chi + O(\beta^2) \end{aligned} \quad (76)$$

Now, if G and $G_{\hat{x}}$ are even functions in χ the second integral on the right hand side will vanish. Not surprisingly, it turns out that all integrands of zeroth order in β are symmetric in χ . Due to the above observations the integration is straightforward and we arrive at:

$$\mathcal{E}_0 = \frac{E(A^{(m)})}{\cos \theta^{(m)}} \quad \mathcal{E}_1 = -\frac{16\theta_{\hat{z}}^{(m)}}{9 \cos \theta^{(m)}} + O(A^2) \quad (77)$$

where $E(A)$ is the energy of a straight soliton of amplitude A integrated over a cross section normal the crest. In terms of the full velocity potential $\phi^{(3)}(\chi, z, A)$, that can be linked to Φ by means of (3), we may write:

$$E(A) = k^{-1} \int_{-\infty}^{\infty} \left[\int_{-1}^{AY} \frac{1}{2} (\nabla^{(3)} \phi^{(3)})^2 dz + \frac{1}{2} A^2 Y^2 \right] d\chi \quad (78)$$

For the vertically integrated flux density we find

$$\vec{f} = (f_0 + \beta f_1) \vec{k}_0 + \beta A B_{\hat{z}} \Phi_0 Y_0 \vec{s} + O(\beta^2, \beta A^{\frac{5}{2}}) \quad (79)$$

where $f_0 \vec{k}_0$ is the contribution from the primary wave and \vec{s} is the unit vector normal to \vec{k} . The last term corresponds to a cross ray energy transport. Physically, this

transport stems from the lateral pressure gradient that necessarily is present under a ridge of variable height and produce lateral accelerations which integrates to a lateral velocity component. The dominant part of the cross ray energy flux then corresponds to the work exerted by the pressure against this velocity. These arguments are easily quantified to enable a direct calculation of the last term of (79) as well as the tangential (\vec{s}) component of the lateral velocity, without application of the formal perturbation expansion. Unfortunately, the other $O(\beta)$ terms cannot be obtained in a similar manner. Integrating the term $f_0 \vec{k}$ we obviously obtain $c_0^{(m)} \mathcal{E}_0 \tan \theta^{(m)}$ due to the consistency of the plane soliton solution. Through integration of the remaining terms in (79) we find a corresponding relation between \mathcal{E}_1 and the integral of f_1 and arrive at:

$$\mathcal{F}_0 + \beta \mathcal{F}_1 = c_0^{(m)} (\mathcal{E}_0 + \beta \mathcal{E}_1) \sin \theta^{(m)} - \beta \frac{4}{3} A_{\hat{s}}^{(m)} + O(\beta^2, \beta A^2) \quad (80)$$

where the index \hat{s} denotes differentiation parallel to the crest (along the $\chi = 0$ contour). The term $\beta c_1^{(0)} \mathcal{E}_0 \sin \theta^{(m)}$ does not show up because it is of higher order in A .

The surface elevation and velocity immediately behind the primary wave is found by putting $x = x^{(m)}$ in (50). When these field quantities are substituted into (75) we find that the leading order in A cancel out and we obtain:

$$\mathcal{D} = \left(\frac{8(\theta_{\hat{s}}^{(m)})^2}{27} + \frac{2(A_{\hat{s}}^{(m)})^2}{3A^{(m)}} \right) \frac{1}{\cos \theta^{(m)}} \quad (81)$$

In view of (23) and (24) we must expect that the two terms are of comparable magnitude. One might object that higher order corrections to $\hat{\eta}$ and $\hat{\phi}$ may be important due to the nihilation of leading contributions to \mathcal{D} . However, a careful examination of the calculation leading to (81) reveals that this is not the case. We further note that the quantity $\cos \theta^{(m)} \mathcal{D}$, which is independent of the orientation of the coordinate axes, can be recognized as the energy leak density measured pr. length of the principal crest.

Summarizing the above results we find the improved energy equation:

$$\begin{aligned} \left(\frac{E}{\cos \theta^{(m)}} - \frac{16}{9} \beta \theta_{\hat{y}}^{(m)} \right)_{\hat{x}} = & - \left(c_0 \tan \theta^{(m)} E - \frac{16}{9} \beta \sin \theta^{(m)} \theta_{\hat{y}}^{(m)} - \frac{4}{3} \beta \cos \theta^{(m)} A_{\hat{y}}^{(m)} \right)_{\hat{y}} \\ & - \frac{\beta}{\cos \theta^{(m)}} \left(\frac{8(\theta_{\hat{y}}^{(m)})^2}{27} + \frac{2(A_{\hat{y}}^{(m)})^2}{3A^{(m)}} \right) \end{aligned} \quad (82)$$

4.3 Higher order ray theory for nearly straight crests.

For gentle deviations from a uniform, straight crest we may assume $\theta^{(m)}$ small. Representing E and c_0 to the leading order in $A^{(m)}$ the energy equation (82) then simplifies to:

$$\{(A^{(m)})^{\frac{3}{2}}\}_{\hat{x}} = -\{(A^{(m)})^{\frac{3}{2}} \theta^{(m)}\}_{\hat{y}} + \frac{\beta}{2\sqrt{3}} A_{\hat{y}\hat{y}} - \beta \frac{(\theta_{\hat{y}}^{(m)})^2}{3\sqrt{3}} - \beta \frac{\sqrt{3}(A_{\hat{y}}^{(m)})^2}{4A^{(m)}} \quad (83)$$

where we also have invoked the lowest order transport equations. The second term on the right hand side has a form akin to the diffusion term of the standard heat

equation, whereas the last term represent an energy sink. Using the same terminology we may classify the first term on the right hand side as an advection term, with $\theta^{(m)}$ in the role as velocity. The corresponding kinematic equation is readily obtained by substituting $c = c_0 + c_1^{(0)}$, with the expression for $c_1^{(0)}$ given by (47), in (20):

$$\theta_{\hat{t}} = -\frac{1}{2}(A + \theta^2)_{\hat{y}} + \frac{\beta}{\sqrt{3}}\{(A^{(m)})^{-\frac{1}{2}}\theta_{\hat{y}}^{(m)}\}_{\hat{y}} \quad (84)$$

Again the corrections of higher order in β give rise to a term of diffusive type in an otherwise hyperbolic equation. We note that no result specific to the “linear fluctuations theory” in section 3.5 has been invoked during the derivation of (83) and (84). A small $\theta^{(m)}$ need not correspond to small relative variations of $A^{(m)}$ as long as $A^{(m)}$ itself is small. Naturally, the errors due to the omission of higher order terms (in A) in E and c_0 will often be larger than the $O(\beta)$ terms in the above transport equations (83) and (84). However, it will still be appropriate to retain the latter terms since they introduce qualitatively new mathematical features. In fact, each term in (83) and (84) can be regarded as the leading representation of a particular physical effect. The tendency toward formation of wave jumps, due to the nonlinear “advective” terms in the transport equations, is now opposed by the diffusion like effect of cross ray energy transport and the dependencies of energy density and propagation velocity upon the curvature of the primary crest.

Under the assumption that all disturbances move along the C^+ characteristic, as defined in (23), the ray description (83) and (84) can be substantially simplified. We further assume that the absolute variations in A is of order β , which imply that the leading nonlinearities (in a defined below) in the “advective” terms of the ray equations are comparable to the “diffusion” like terms. Consequently, we change variables according to:

$$A = A_0(1 + \beta a) \quad \theta = \beta A_0^{\frac{1}{2}}\psi \quad \hat{y} = A_0(\hat{y} - U\hat{t}) \quad (85)$$

where $U = \sqrt{A_0/3}$ is introduced according to (23). In the new frame of reference, that is moving with the “linear” modulation velocity U , we may now assume that the time dependence can be represented by the second order slow variable:

$$\tau = \beta U A_0 \hat{t} = \beta^2 U A_0 t \quad (86)$$

Inserting the new variables into (83) and (84) we obtain, after some manipulation, a relation between ψ and a :

$$\psi = \frac{\sqrt{3}}{2}a - \frac{\sqrt{3}}{2}\beta\left(\frac{1}{4}(a^2) + \frac{1}{3}a_{\hat{y}}\right) + O(\beta^2) \quad (87)$$

and a Burgers’ equation for a :

$$a_{\tau} + (a^2)_{\hat{y}} - \frac{2}{3}a_{\hat{y}\hat{y}} = O(\beta) \quad (88)$$

We note that the leakage term has dropped out of the equation to the present order.

In section 3.5 we found, to leading order in β and $A - A_0$, that a progressive perturbation produce a plane and uniform diffracted waves of length $O(\beta^{-1})$. If higher order terms is taken into account, as in (88), the shape of the diffracted wave will evolve at a rate of order β^2 . Thus, the diffracted wave field may be regarded as a slowly varying solution of the linear hydrostatic equations.

4.4 Higher order equations for radially converging waves

The symmetric case can not inherit the diffusion like features of the nearly straight crests discussed in the previous subsection. However, both the energy density and the wave celerity speed do still depend on the gradient of A and the energy leak due to diffracted waves will also remain. The energy transport equation may now be formulated simply as a balance between energy loss in the principal wave and energy accumulated in the trailing wave system that is continuously prolonged. We may derive the equation either as an offspring of (82) or by direct application of energy arguments. Choosing the latter and still confining ourselves to in-going waves, we find:

$$(r^{(m)}\mathcal{E})_{\dot{t}} = -\beta r^{(m)}(c_0 - 1)\hat{\eta}_{-\infty}^2|_{r=r^{(m)}} + O(\beta^2, \beta A^2) \quad (89)$$

where $\mathcal{E} = E + \beta \frac{16}{9r^{(m)}}$ and $\eta_{-\infty}$ is as defined in section 3.4. Inserting the unified solution of section 3.6 for $\eta_{-\infty}$ and exploiting the dominant balance inherent in (89) we may rewrite this equation in an integrable form. In terms of fast variables only we find:

$$r^{(m)}E + \frac{16}{9} - \frac{8}{27} \ln r^{(m)} = \text{const.} \quad (90)$$

We note that the contribution from the $O(\beta)$ part of \mathcal{E} turn out to be constant. Introduction of a reference state $r^{(m)} = r_0$, $A^{(m)} = A_0$ leads to:

$$r^{(m)}E(A^{(m)}) = r_0E(A_0) + \frac{8}{27} \ln \frac{r^{(m)}}{r_0} \quad (91)$$

that combined with the kinematic equation:

$$r_{\dot{t}}^{(m)} = -c_0^{(m)} \left(1 + \frac{1}{\sqrt{3A^{(m)}r^{(m)}}}\right) \quad (92)$$

defines $A^{(m)}$ and $r^{(m)}$ as functions of t . The equations (91) and (92) are described exclusively in terms of fast variables with $r^{(m)}$ itself as the ordering parameter. This reflects that the underlying perturbation expansion is asymptotically valid for large r . As the wave approach the point of symmetry the right hand side of (91) is bound to change sign for some $r^{(m)}$ and the equation loose sense. However, the whole asymptotic solution will become invalid long before this point is reached.

Ko & Kuehl (1979) report an amplitude evolution that is consistent with having the logarithmic term of (91) multiplied by $r^{(m)}$. This leads to meaningless results and is certainly due to a misprint.

As opposed to the case of gently perturbed crests the curvature dependence in the energy density introduces no principally new features in the final energy equation (91). This would probably still be the case even if \mathcal{E}_1 was calculated to the next order in A . We are then left with the energy loss to the diffracted tail as the genuine first order effect in β . This effect is generally very small and may be important only when accumulated over an extremely large propagation distance.

The significance of the diffraction is illustrated in figure 2 where we have depicted results from (91). Waveheights of the primary crest, $H \equiv AY(0, A)$, are displayed for three different levels of approximation:

- (i) The diffraction term is retained, $E = \frac{8}{3\sqrt{3}}A^{\frac{3}{2}}$ is used for the integrated energy density and H is set equal to A , corresponding to the approximation: $Y \approx Y_0$.

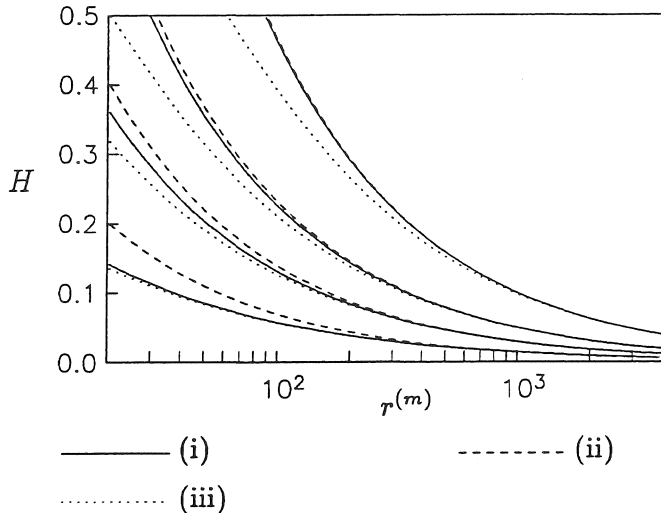


Figure 2: Height of primary wave, $H = A^{(m)}Y(0, A^{(m)})$ versus $r^{(m)}$ for different approximations to 91 as explained in the text.

- (ii) As previous point, except that the logarithmic diffraction term is omitted.
- (iii) The diffraction term is retained and we have invoked the corrected representations:

$$E(A) = \frac{8}{3\sqrt{3}}A^{\frac{3}{2}}(1 + \frac{33}{20}A) \quad Y = Y_0 + \frac{3}{4}AY_0^2$$

where the higher order terms are obtained by combining expansions for energy integrals given in Longuet-Higgins & Fenton (1974) and expansions for the surface elevation in Laitone (1960).

In the figure we have depicted the $H(r^{(m)})$ curves for the reference position $r_0 = 1000$ and the reference waveheights: $H_0 = 0.1, 0.05, 0.03, 0.015$. It is apparent that the energy leak dominates over higher order contributions to E only for the case corresponding to the smallest reference waveheight. Regarding comparison to numerical solutions we may thus expect improved agreement due to the diffraction term in (91) for the domain in the H - $r^{(m)}$ plane close to or below the lowest curve in the figure. We also see that the leading representation of E yields good results for $A < 0.25$, say.

Finally we note that for small A the equation 91 applies equally well when A is replaced by the total waveheight, $\eta_{\max} \equiv \max(AY + \beta\hat{\eta})$. The explanation is simply that we to the appropriate order have $r^{(m)}(A^{(m)})^{\frac{3}{2}} - r^{(m)}(\eta_{\max})^{\frac{3}{2}} = \text{const.}$

5 Examples

We will study the evolution of inhomogeneous solitary crests for three particular cases. Each case is analyzed by the present optical theory as well as another method that involves no assumption of slow variation. In addition to the description of the primary crest, represented by $\theta^{(m)}$ and $A^{(m)}$, we will pay attention also to the diffracted wave fields and energy flux distributions.

First we study a progressive perturbation corresponding to a self-similar solution of the Burgers equation (88) that describes the evolution of the junction between two dislocated, but otherwise identical, semi-infinite crests. This solution is compared to numerical solutions of the Boussinesq equations and the set (83) and (84).

The second example is a wave jump of permanent form for which we compare results from the ray description to the general solution for a triad of solitons reported by Miles (1977b). The comparison provides a valuable verification of the validity of the ray equations derived herein. Also this example concerns a transition between two straight crest, but this time a net change in orientation and amplitude is involved.

Finally we investigate a crest with radial symmetry. Mathematically this is a one dimensional problem for which we may compute very accurate solutions from the Boussinesq equations, permitting discussion of quantities like $c_1^{(0)}$. Since the ray theory in this case can be regarded as an asymptotic approximation for large r incoming waves provide well suited test examples for which the basic assumptions become gradually strained as $r^{(m)}$ diminish with time.

5.1 A self-similar perturbation – comparison to the Boussinesq equations

The numerical procedure for solution of the Boussinesq equations differ from the one applied in Pedersen (1988) only with regard to minor, technical details. Consequently, we omit the description of the method. The ability of the method to represent solitary waves is studied by Pedersen (1989), who demonstrated the existence of discrete solitary waves expressible as single crested permanent form solutions of the difference equations. This is important in the present context where both length and time scales for the development of wave patterns may be very large and even a slight spurious damping or disintegration may corrupt the results. The transport equations (83) and (84) are of the mixed hyperbolic/parabolic type that is so beloved by authors of textbooks on numerical solution of partial differential equation. For completeness we sketch the method in the appendix. To enable comparison with ray theory some secondary unknowns have to be calculated from the discrete Boussinesq solution. Energy fluxes are found by numerical integration of discrete counterparts of the expression:

$$\vec{f} = -\bar{\phi}_t(1 + \eta)\nabla\bar{\phi}(1 + O(\epsilon^2, \alpha\epsilon)) \quad (93)$$

The height and position of the primary crest are determined by finding the extremes of spline interpolants defined along grid rows parallel to the x -axis. Strictly, we may define the crest peak as the set of maximum points for η at curves normal to the contour lines of η . Thus, for a non-uniform crest the ridge locations and heights from the spline interpolants should be modified. Observing that these modifications are small (due to the long scale of the non-uniformity) corrections are easily found through employment of geometrical considerations and the soliton solution. For the cases reported herein they turn out to be negligible. Another point is the deviation between A as defined in the perturbation expansion, and thereby in the ray equations, and the maximum of the full soliton solution. However, ignoring the difference is an approximation similar to (16) that is invoked also during the derivation of (83) and (84). Also the higher order shape correction $\hat{\eta}$ will modify the relation between A and the maximum wave height, but this is hardly noticeable for the comparisons within

the present subsection. On the other hand, regarding the check on the expression (47) for $c_1^{(0)}$ performed for the axisymmetric case in 5.3 this point will be crucial. The angle of orientation, $\theta^{(m)}$, is found by a polynomial (usual cubic) least square fit to the interpolated extremes. Since the position of a maximum is sensitive to errors this procedure may sometimes produce visible artificial fluctuations, but generally not to an extent that affects the interpretation of the results.

We will attach a few further comments on the wave patterns predicted by the Boussinesq equations. As shown in the preceding sections the Boussinesq equations reproduce $\hat{\eta}$, $\hat{\phi}$ and c_1 correctly to the leading order in A . Also the simple energy equation (18), that may follow from (45), is inherent in this description. However, since the Boussinesq equations are not exactly energy conserving the corrected energy equation (83) can not automatically be anticipated to apply to their solutions. Still, we would expect improved agreement from the higher order transport equations as we indeed will observe. The initial conditions are derived from an initial distribution of $A^{(m)}(y)$ and $\theta^{(m)}(y)$ by substituting a phase function $\chi_{in}(x, y) \equiv k^{(m)} \cos \theta^{(m)}(x - x^{(m)})$ into the exact soliton solution for the actual Boussinesq equations. This solution is given in Pedersen (1988). Consequently, neither the full spatial variation of A and θ nor the $O(\beta)$ wave field are present in the initial state, but will evolve in time. The error introduced in this manner is small, while the fact that the secondary wave fields are spontaneously induced over time increase their value as evidence for the ray theory.

The Burgers equation, that is a standard model equation for combining effects of nonlinearity and diffusion, can be transformed to the linear heat equation by means of the Cole-Hopf transformation. Both the equation itself, the transformation and a selection of analytical solutions are discussed in detail by Whitham (1974). Here we will employ a self-similar solution that can be expressed in the variables y and t according to:

$$\left. \begin{aligned} \frac{A^{(m)} - A_0}{A_0} &= \frac{\Delta_{\max}(t/t_0 + 1)^{-\frac{1}{2}} e^{\sigma_{\max}^2 - \sigma^2}}{1 + \frac{3A_0 L}{2\sqrt{\ln 2}} \Delta_{\max} e^{\sigma_{\max}^2} (\operatorname{erf}(\sigma_{\max}) - \operatorname{erf}(\sigma))} \\ \sigma &= \frac{\sqrt{\ln 2}(y - Ut)}{L\sqrt{t/t_0 + 1}} \quad t_0 = \frac{3\sqrt{3}A_0 L^2}{8 \ln 2} \quad \sigma_{\max} = \frac{3A_0 L}{4\sqrt{\ln 2}} \Delta_{\max} \end{aligned} \right\} \quad (94)$$

where U is as defined in (85) and erf denotes the error function. The solution contains two free parameters: Δ_{\max} that is the maximum initial relative perturbation of the amplitude, attained at $\sigma = \sigma_{\max}$, and L that is a measure of the initial lateral extension of the perturbation.

In figure 3 we have depicted the solutions of the characteristic equations (23), (24) and the Boussinesq equations for initial conditions corresponding to (94) with $A_0 = 0.1$, $\Delta_{\max} = 0.15$ and $L = 66.7$. Although there are good agreement for the propagation speed of the disturbance, the different qualitative behavior of the two solutions is striking. The solution of the simple ray equations steepens and become rapidly double valued even though the initial perturbation is very gentle, whereas the Boussinesq solution instead displays a substantial damping and spreading in line with the time evolution of the self-similar solution (94). As shown in figure 4 there are also close quantitative agreement between the solution of the Burgers equation, (94), the solution of the Boussinesq equations and the numerical solution of the set (83) and (84) with the leak term intact. Omitting the last term in (83) we observe only very small changes in the solution; θ being altered typically 0.01° . As compared

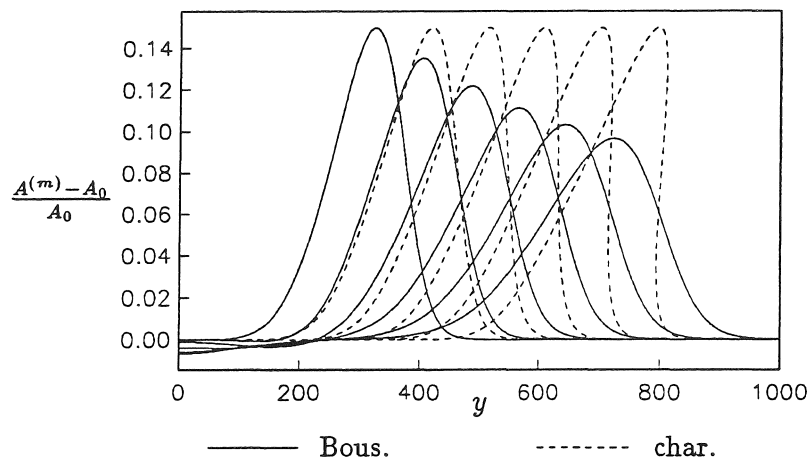


Figure 3: Time development of the initial condition (94) with parameters $A_0 = 0.1$, $\Delta_{\max} = 0.15$ and $L = 66.7$. The selected times are $t = 0, 400, 800, \dots, 2000$. The dashed lines correspond to the solution of the characteristic equations ((23) and (24)), whereas the numerical solution of the Boussinesq equations is depicted with solid lines.

to the higher order ray solutions the Boussinesq equations yield to high perturbation amplitudes and to small angles. However, the difference evolves mainly during the first part of the simulation, whereas the succeeding trends are quite similar. Thus, the deviations probably stem mainly from the different relations between A and θ that is inherent in the different descriptions of the unidirectional progressive modulations.

In figure 5(a) we have depicted the y -component of the integrated energy flux associated with the primary crest, which is the quantity denoted by \mathcal{F} in section 4.2. The integration of the numerical solution is performed over the interval $x^{(m)} - D < x < x^{(m)} + D$ where D is defined according to $Y_0(k^{(m)}D) = 10^{-3}$. There are close agreement between (80), substituted (77) and (16), and the integrated flux from the Boussinesq solution. The cross ray energy flux components, defined as normal to $\vec{n}^{(m)}(y, t)$ at the actual y -location, and still integrated within the width of the primary wave, are displayed in figure 5(b). Again we find convincing agreement, particularly in view of the two levels of interpolation that are involved.

Concerning the higher order (in β) contributions to the wave field it is very difficult to extract the form correction of the primary wave from the Boussinesq solution due to its small magnitude compared with discretization and interpolation errors. The cross ray velocity component, $u^{(s)}$, is on the other hand of order β throughout the wave field and can thus be computed also within the primary wave. Still the definition of cross ray is as given above. From the definition (25) of the velocity potential we then find:

$$u^{(s)} = (B_y \Phi_0 + Bk(\theta - \theta^{(m)})Y_0)(1 + O(\beta, \theta^2, A_0)) \quad (95)$$

We evaluate this expression by extracting $A^{(m)}$ and $\theta^{(m)}$ from the Boussinesq equation and apply the continuation, given in section 3.5, to the complete A and θ field. As shown in figure 6 the result of this procedure agrees excellently with values directly

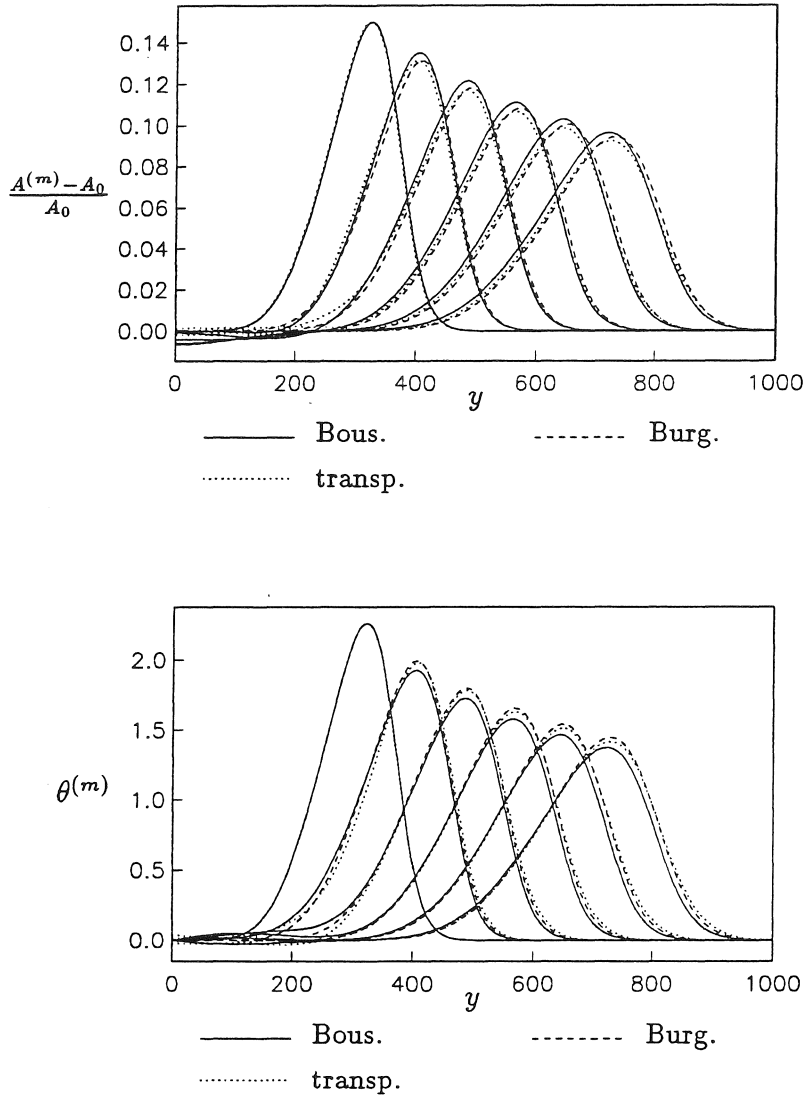


Figure 4: Time development of the initial condition (94) with parameters $A_0 = 0.1$, $\Delta_{\max} = 0.15$ and $L = 66.7$. The selected times are $t = 0, 400, 800, \dots, 2000$ and $\theta^{(m)}$ is measured in degrees. The numerical solution of the Boussinesq equations is depicted with solid lines, the dashed lines correspond to the Burgers equation (88) and the dotted line represent the solution of the transport equations (83) (84) with the leak term intact.

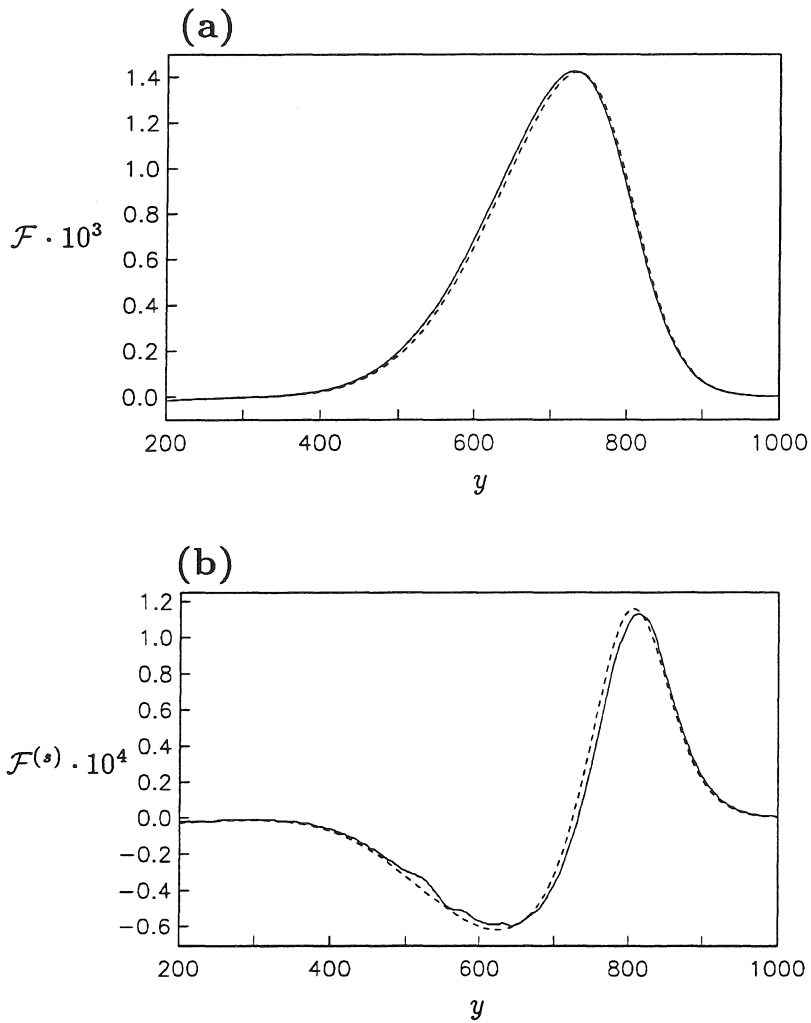


Figure 5: *Integrated energy fluxes for the case displayed in figure 4 after $t = 2000$. (a): The y component of the flux associated with the leading crest. (b) The cross-ray component for the primary crest. Fluxes from the Boussinesq solution are represented by solid lines. The dashed lines correspond to fluxes obtained by substituting the interpolated amplitudes and orientations from this solution into the terms on the right hand side of (80), using the approximation (16) for E .*

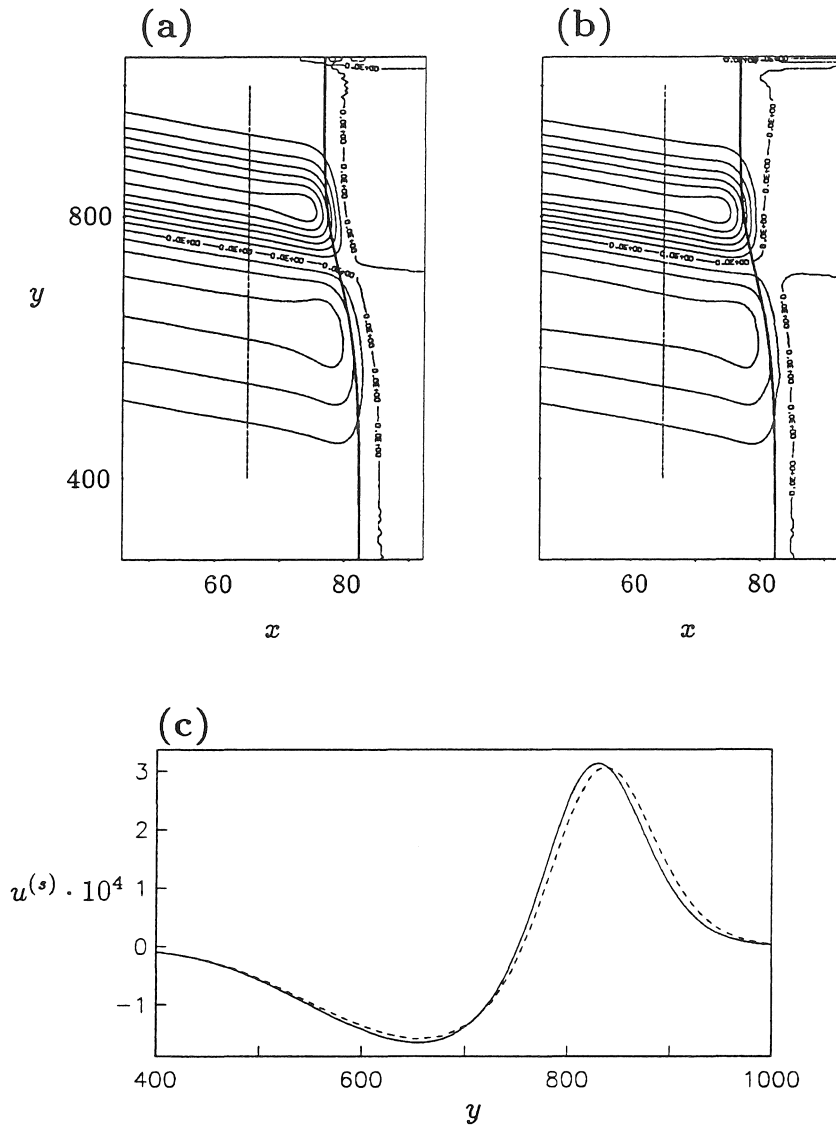


Figure 6: Cross ray velocities for the case displayed in figure 4 after $t = 2000$.
 (a): Contour plot of $u^{(s)}$ obtained from (95) and results of section 3.5. (b): Interpolated $u^{(s)}$ from Boussinesq solution. The contour increment is $0.5 \cdot 10^{-4}$, the relative stretch of x scale is 10, the fat solid line corresponds to the position of the peak and the vertical lines at $x = 65$ displays the cross-sections depicted in (c). The visible difference in orientation corresponds roughly to $\tan \theta_d - \theta_d$.
 (c): u_s at the cross-section $x = 65$. The solid and dashed lines represent the Boussinesq solution and (95) respectively.

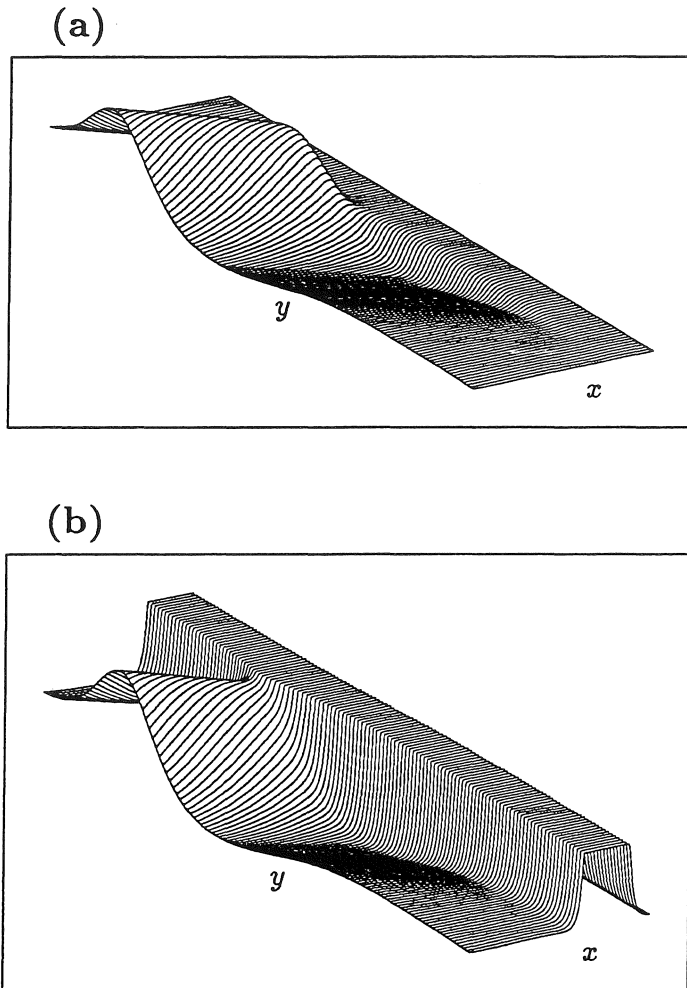


Figure 7: The surface elevation of the diffracted wave for the case displayed in figure 4 after $t = 2000$.

(a): $\beta\hat{\eta}$ based on interpolated values for $A^{(m)}$ and $\theta^{(m)}$. (b): The Boussinesq solution. The x and z axes are stretched relative to the y -axis, the view point is behind the leading crest and the flat narrow shelf in (b) is the primary wave that has been cut off at $z = 0.7 \cdot 10^{-3}$.

interpolated from the Boussinesq solution. The surface elevation of the residual wave field are depicted in figure 7. The diffracted wave system mainly consists of a crest, originating from the part of the primary stem with positive $\theta_y^{(m)}$, followed by a trough associated with regions of negative $\theta_y^{(m)}$. For the orientation of the diffracted wave field we find $\theta_d \approx 30^\circ$. The deviations from the result $\theta_d = \sqrt{3A_0} = 31.4^\circ$ of section 3.5 is of the same order as in approximations like $\sin \theta_d \approx \theta_d$ that are frequently used throughout the actual calculations.

We will end this section by the study the behavior of an relative abrupt change in $x^{(m)}$ corresponding to $A_0 = 0.1$, $L = 8$ and $\Delta_{\max} = 1$. This case must be expected to fall beyond the limits of the ray theory, at least for small t . Still, as shown in figure 8, we observe the same qualitative behavior as in the previous cases with a dominant extension of the transition zone over time. Even the quantitative agreement between the transport equations and the Boussinesq equations is quite good. The diffusion like spreading are much stronger than for more gentle modulations which suggest that these effects may be more important outside the slowly varying regime than within. This time the diffraction term has a marked influence upon the solution of (83) and (84) (10% in a), but the picture is by no means dominated by diffraction effects.

5.2 Wave jump – comparison to Miles solution

According to (23) and (24) shocks, in the sense of discontinuities of wave characteristics, will evolve from any initial perturbation of a crest. These are crude representations of wave jumps that often can be initiated by a nonuniform geometry. A familiar example of the latter is a vertical wall with a concave corner at which a Mach reflection pattern may start to evolve. Kulikovskii & Reutov (1980) and Liu & Yoon (1986) report wave jumps generated at trenches for solitary and Stokes' waves respectively. The diffusion like terms of (84), (83) or (88) must be expected to inhibit development of discontinuities and instead yield more detailed descriptions of jumps of finite width.

Shock solutions of ray equations for solitary waves, similar to (23), (24), are discussed in Miles (1977c) and Kulikovskii (1976,1980). A more complete discussion of a jump, in the sense of an relative abrupt change in amplitude and orientation of the carrier wave, is found in Miles (1977b) which is the second paper of a pair presenting an excellent analysis of obliquely interacting solitons. In that context the shock is described as a phase locked triad for which analytical solutions are presented. These solutions are accurate to the same order as the Boussinesq equations. A definition sketch of such a triad is shown in figure 9 where the dashed line corresponds to the member of the triad that is not inherent in the lowest order (pure hyperbolic) ray theory. The pattern is completely determined by the amplitude at one side of the shock and the jump in orientation, corresponding to θ_i in figure 9. Using the conventions implicit in the figure, we may write the asymptotic relations of Miles solution as:

$$\left. \begin{aligned} A_w &= A_i \left(1 + \frac{A_i^{-\frac{1}{2}} \theta_i}{\sqrt{3}} \right)^2 & U_m &= \sqrt{\frac{A_i}{3}} \left(1 - \frac{2}{\sqrt{3}} A_i^{-\frac{1}{2}} \theta_i \right) \\ A_r &= \frac{1}{3} \theta_i^2 & \theta_r &= \sqrt{3A_i} \end{aligned} \right\} \quad (96)$$

where A_i and A_w are the amplitudes ahead and behind of the jump respectively, while A_r and θ_r define the characteristics of the third wave. From the ray theoretical point

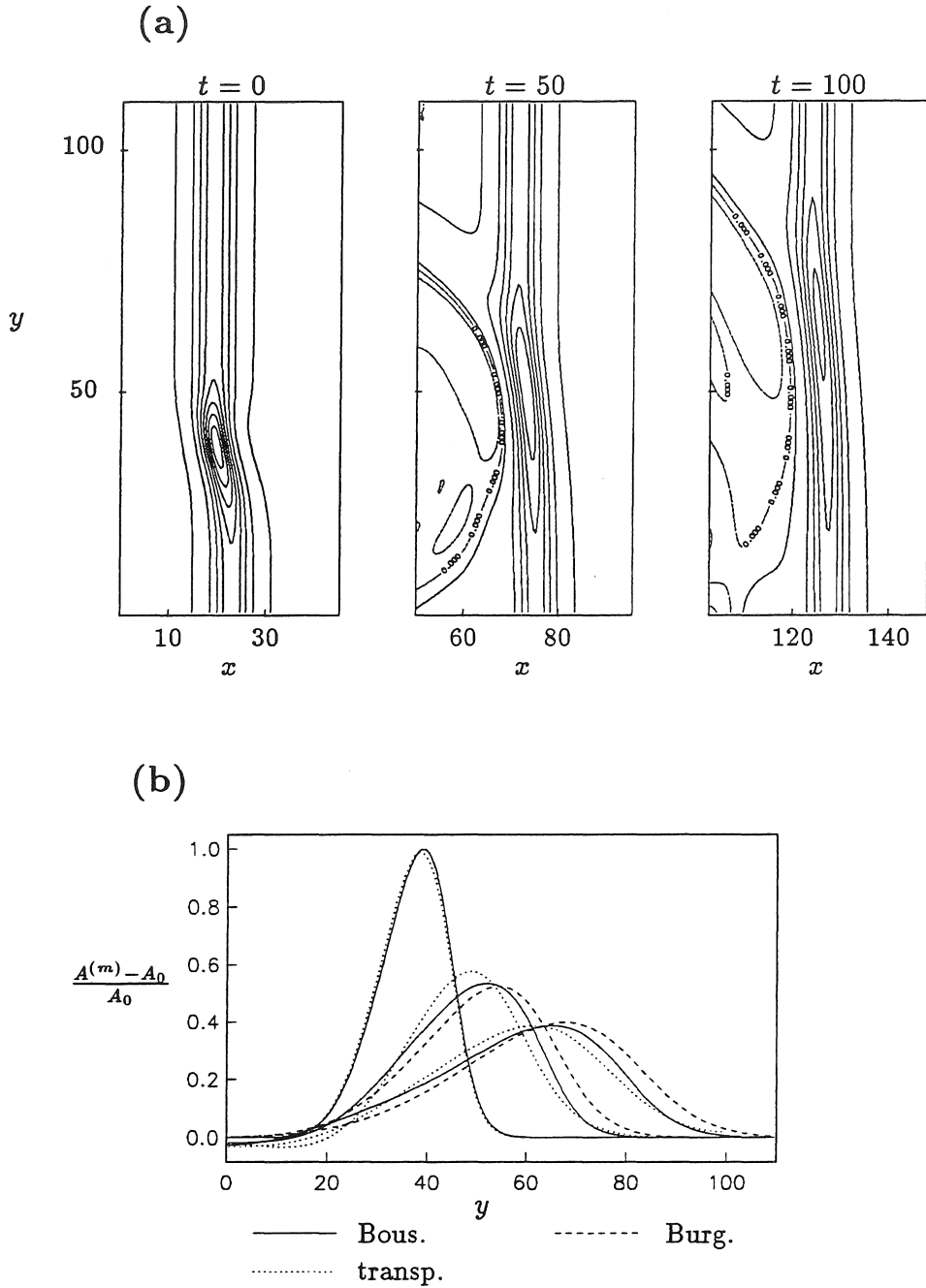


Figure 8: The development of a short nonuniform region, defined according to $A_0 = 0.1$, $\Delta_{\max} = 1$ and $L = 8$.

(a): Contour plot of η obtained by numerical integration of the Boussinesq equations, with 0.025 as contour increment and equally scaled axes.

(b): Amplitudes calculated by the different equations for $t = 0, 50, 100$. The interpretation of the curve types is as in figure 4 and the discrepancies at $t = 0$ are due to interpolation errors.

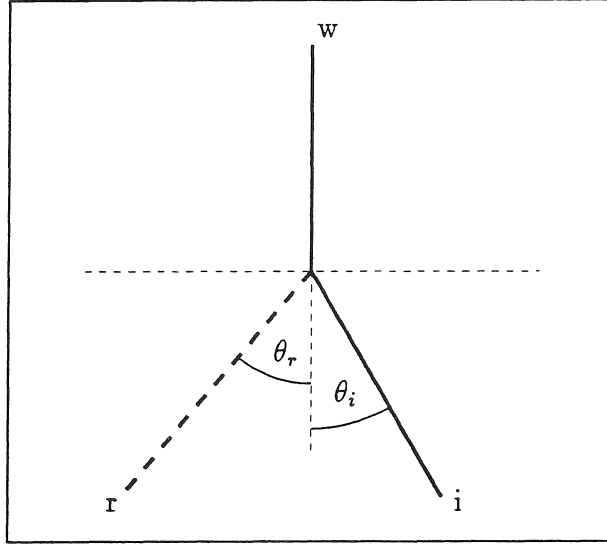


Figure 9: A phase locked triad. The triple point (shock) moves downward and the dashed line presents the weakest member of the triad. The pattern is oriented like a Mach reflection pattern to make the letters i , r and w denote the incident, stem and reflected wave respectively.

of view the presence of the latter can be regarded as diffraction from the jump zone. After rescaling according to (15) the surface elevation of Miles solution reads:

$$\frac{1}{4}\eta = \frac{A_i e^{4\chi_w - 2\chi_i} + A_w e^{2\chi_w} + A_r e^{2\chi_r}}{(1 + e^{2\chi_w} + e^{2\chi_r})^2} \quad (97)$$

where the phases are given according to:

$$\chi_i = \frac{\sqrt{3A_i}}{2}(\cos \theta_i(x - x_f) + \sin \theta_i(y - y_f)) \quad \chi_w = \frac{\sqrt{3A_w}}{2}(x - x_f) \quad \chi_r = \chi_w - \chi_i \quad (98)$$

and the values of x_f and y_f determine the location of the triple point. It is easily deduced that the shock width is proportional to θ_i^{-1} . Thus, provided $A_i^{-\frac{1}{2}}\theta_i \ll 1$ the Burger equation (88) should reproduce the above jump relations to leading order. The diffracted wave can then be calculated by means of (50) and (56). First we note that the angle θ_r from (96) is identical to the general angle of diffracted wave systems that was found in section 3.5. Next, finding a permanent jump solution of (88) and re-inserting the scaling (15) we obtain:

$$A = A_i \left(1 + \frac{1}{\sqrt{3}} A_i^{-\frac{1}{2}} \theta_i \left(1 + \tanh \left(\frac{\sqrt{3}}{2} A_i^{\frac{1}{2}} \theta_i (y + U_s t) \right) \right) \right) \quad (99)$$

where the shock speed U_s is as given in (96). However, the shock speed depends solely on the asymptotic characteristics of the jump (A_i , A_w and θ_i) and is not affected by the diffusion-like terms of the corrected ray theory. The jump profile, on the other hand, is crucially dependent on these terms and does coincide with Miles solution in the limit $A_i^{-\frac{1}{2}}\theta_i \rightarrow 0$, $A_i \rightarrow 0$. This is most easily demonstrated through calculation of the diffracted wave (sec. 3.5) that to leading order becomes a soliton with amplitude equal to A_r as given in (96). The asymptotic agreement with Miles solution clearly demonstrates the validity of the present theory.

In figure 10 we have displayed $A^{(m)}$ for two jumps, corresponding to $A_i = 0.05$, $\theta_i = 0.5^\circ$ and $A_i = 0.02$, $\theta_i = 7^\circ$ respectively. Whereas the first case yields a large jump width, the validity of the ray description is more questionable for the latter. However, even for the second case we obtain rather good results from the transport equations (83) and (84).

5.3 Axisymmetric converging waves

Propagation and evolution of axisymmetric waves in the weakly nonlinear and dispersive regime has been the topic of several papers as Cumberbatch (1978) and Miles (1977d). Ko & Kuehl (1979) reported a perturbation technique closely related to the present (see sec. 3.2). They found good agreement between their analytical results and numerical simulations concerning the amplification of focusing cylindrical and spherical waves. However, no detailed comparison for the wave profiles were presented.

The main objective of the present study of focusing waves is to seek direct verification of the representations of $\hat{\eta}$ and $c_1^{(0)}$ in section 3 through comparison to accurate numerical solutions of (7) and (8).

The variable coefficients of these Boussinesq type equations introduce no difficulties concerning numerical solution, apart from the extra caution required to resolve the neighborhood of $r = 0$. We apply a straightforward generalization of the method in Pedersen (1988) for which any further description should be superfluous. For each numerical calculation the discretization errors are estimated by grid refinement tests. The values for height, η_{\max} , and position, r_{\max} , of the crest peak are generally improved through a simple extrapolation routine that utilize the second order (in grid increments) convergence of the numerical method.

To the significant order the combination of (13), (25), (65) and (66) gives the following relation between r_{\max} , η_{\max} and A , $r^{(m)}$:

$$\eta_{\max} = H + \frac{2}{3r^{(m)}\sqrt{3A^{(m)}}} \quad r_{\max} = r^{(m)} + \frac{2}{3r^{(m)}(A^{(m)})^2} \quad (100)$$

where the height of the primary wave is given as $H = AY(0, A)$. When η_{\max} and r_{\max} are found from the numerical solution the above equations can be inverted to yield $A^{(m)}$ and $r^{(m)}$, whereafter the whole perturbation solution can be calculated at the given instant. In the comparisons that are to follow we use exact representations, belonging to the Boussinesq equations, for Y and c_0 as functions of H .

In figure 11 we have compared the amplification in a numerical simulation to the predictions of (91). The numerical integration was started with $H_0 = 0.0198$, $r_{\max} = 4000$ and initial conditions corresponding to the exact plane soliton solution of the Boussinesq equations. However, the comparison is started when $r_{\max} < 3000$ and the wave pattern presumably is nearly fully developed. The agreement is as least as good as can be expected in view of the results in figure 2. According to the same figure we should not emphasize the improved agreement due to the leak term for this case. Wave profiles for $t = 3400$ are compared in figure 12. We observe that the contribution from $\hat{\eta}$ is significant and that the unified solution agrees well with the numerical solution for the crest as well as the diffracted tail. Again we note that the secondary characteristics of the wave system evolve spontaneously during the numerical integration. The most pronounced deviations are found at the head

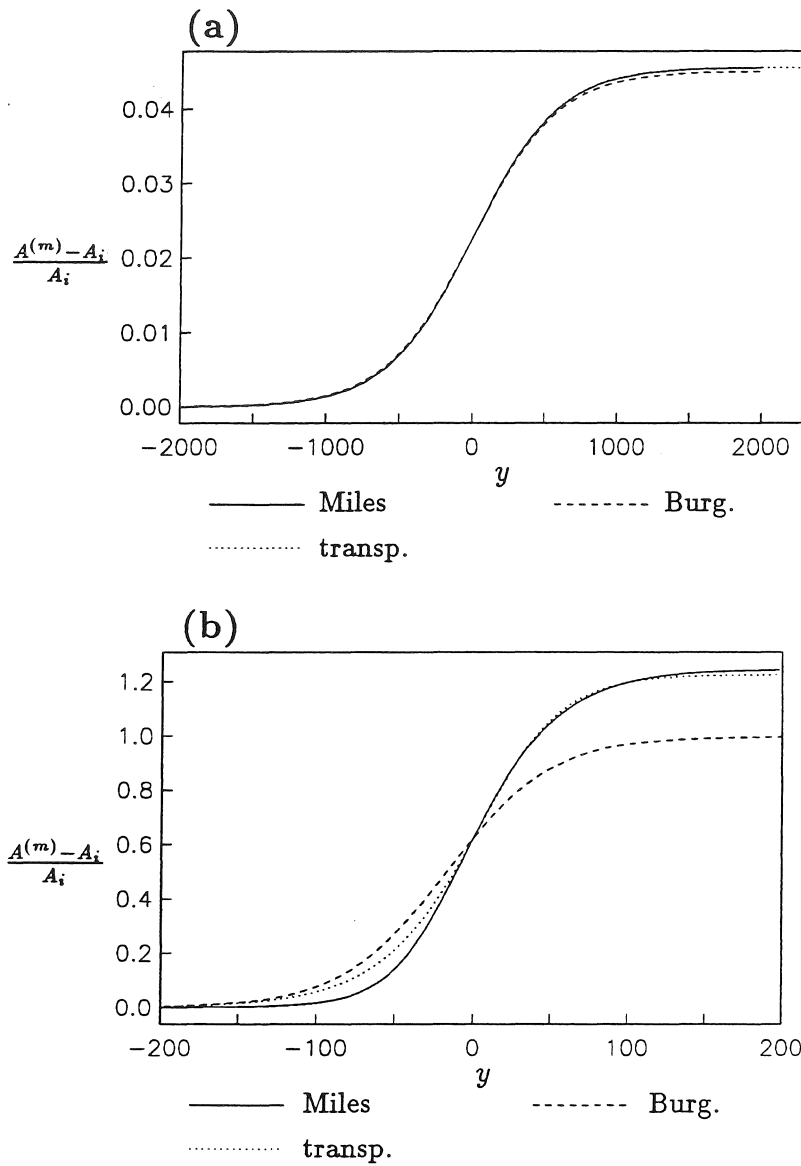


Figure 10: The variation of the amplitude, $A^{(m)}$, across wave jumps.

(a): $A_i = 0.05$ and $\theta_i = 0.5^\circ$, (a): $A_i = 0.02$ and $\theta_i = 7^\circ$.

The jump solution of Miles is depicted with solid lines, the dashed lines correspond to the Burgers equation (88) and the dotted lines represent the solution of the transport equations (83) (84) with the leak term intact. We have chosen the position where Miles solution predicts $A^{(m)} = \frac{1}{2}(A_i + A_w)$ as origin.

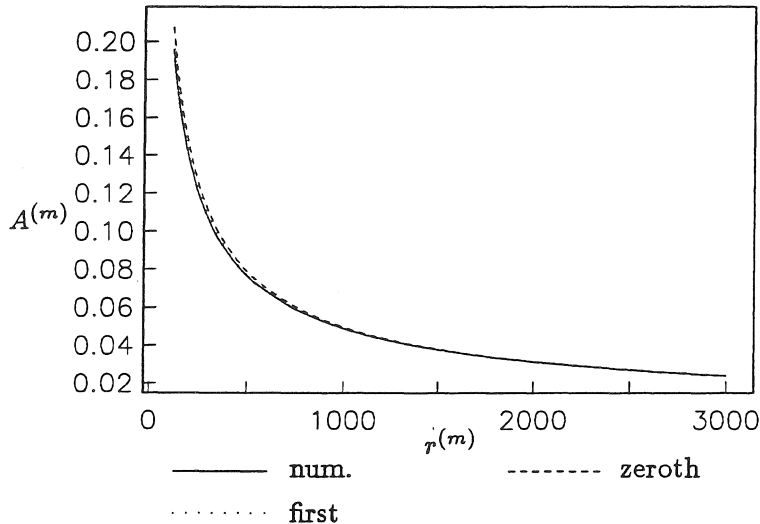


Figure 11: $A^{(m)}(r^{(m)})$ for a radially converging wave with initial conditions corresponding to a plane soliton solution with parameters $r_0 = 4000$, $H_0 = 0.0198$. We have depicted the numerically calculated amplitude (num.), the amplitude from (91) without the leak term (zeroth) and the amplitude predicted by the complete equation (91) (first). The energy equation (91) is applied with the modified reference point $r_0 = 2999.8$, $A_0 = 0.0239$ to avoid the effect of inaccurate initial conditions.

of the tail where the numerical solution displays some weak ondulatory behavior. This feature resemble the tail generated when a plane soliton evolves from a slightly perturbed initial condition and is significantly altered neither by invoking the full perturbation solution as initial conditions, starting the soliton from a larger r_{\max} or by refining the grid. We are thus led to suggest that ondulations reflect the “struggle” of the primary wave to preserve its identity and solitary shape. It is not clear to what extent these effects may be included through higher order terms of the perturbation expansion. The expressions (68) and (69) give equally good agreement for the leading crest as the unified solution, but do not reproduce the tail.

Whereas the factor $c_1^{(0)}$ was essential for the appropriate description of wave jumps in the preceding section, it is of minor importance in the context of axisymmetric waves. On the other hand, numerical solutions for radially converging waves provides an excellent opportunity for direct validation of the expression (47). Given $H(t)$ and $r^{(m)}(t)$, as extracted from the numerical solution, we may calculate the inherent errors in two anticipated positions according to:

$$\Delta r_0 = r^{(m)}(t_1) - \int_{t_1}^t c_0(H) dt - r^{(m)} \quad \Delta r_1 = \Delta r_1 - \int_{t_1}^t \frac{c_0}{r^{(m)} \sqrt{3H}} dt \quad (101)$$

where c_0 is the exact soliton speed belonging to the Boussinesq equations and the second integrand is recognized as $c_1^{(0)}$ for the radially symmetric case. For the same case as above we have displayed the two dislocations in figure 13. It is clear that the retainment of $c_1^{(0)}$ reduces the error by an order of magnitude.

Finally, in figure 14, we have depicted the amplification of a wave with initial parameters $r_0 = 6000$, $\eta_{\max} = 0.005$ that roughly correspond to the lowest curve in

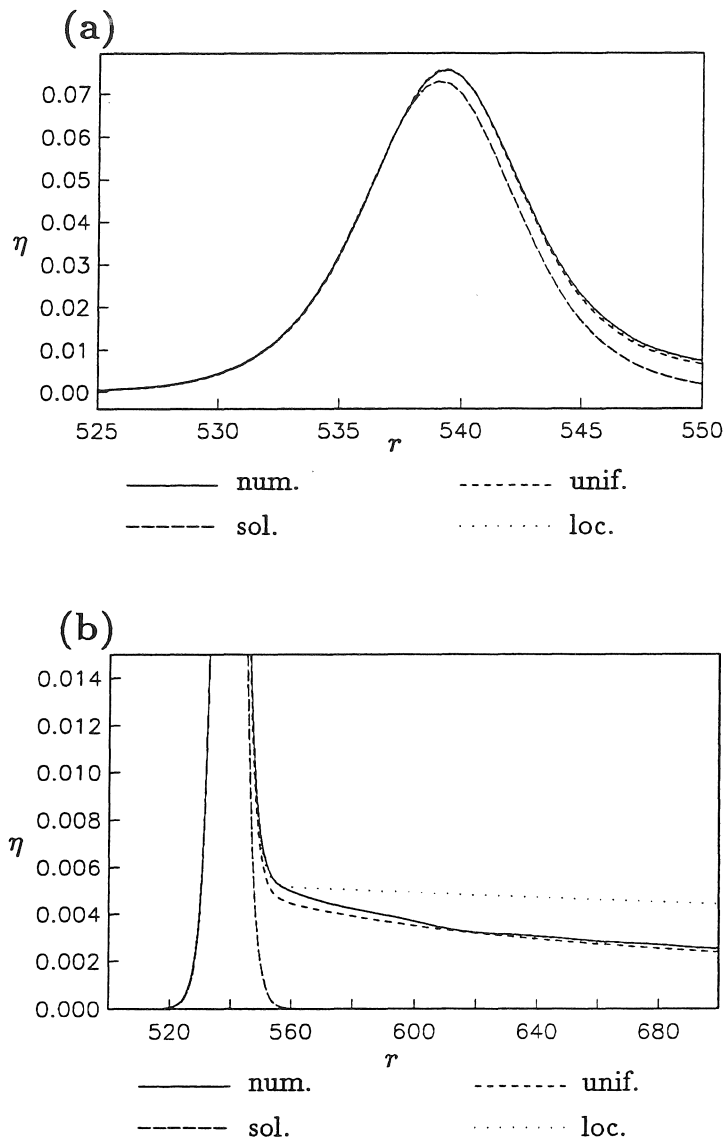


Figure 12: Surface elevation at $t = 3400$ for a radially converging wave with initial conditions corresponding to a plane soliton solution with parameters $r_0 = 4000$, $A_0 = 0.0198$. We have depicted the numerically calculated surface elevation (num.), the unified perturbation solution (unif.) defined by (65) and (66), the soliton profile (sol.) and the local perturbation solution (loc.) defined by (69) and (68). The last three curves are based on the location and size of the maximum surface elevation in the numerical Boussinesq solution.

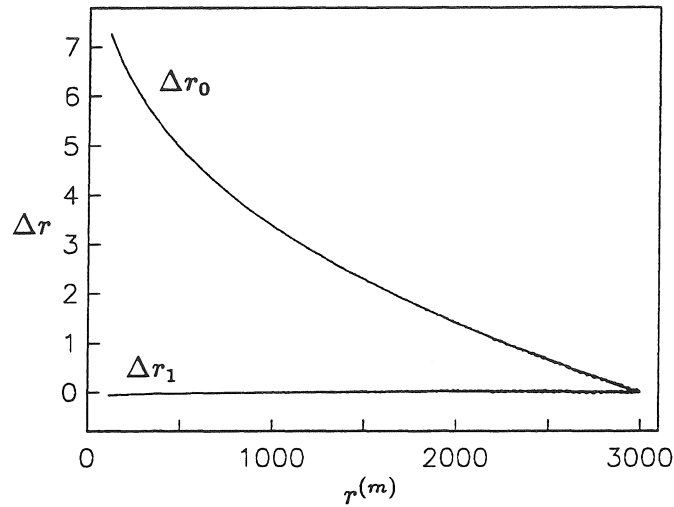


Figure 13: Errors for zeroth and first order approximation, in term of β , to $r^{(m)}$ as given in (101). The flossy appearance of the curves is probably due to interpolation errors.

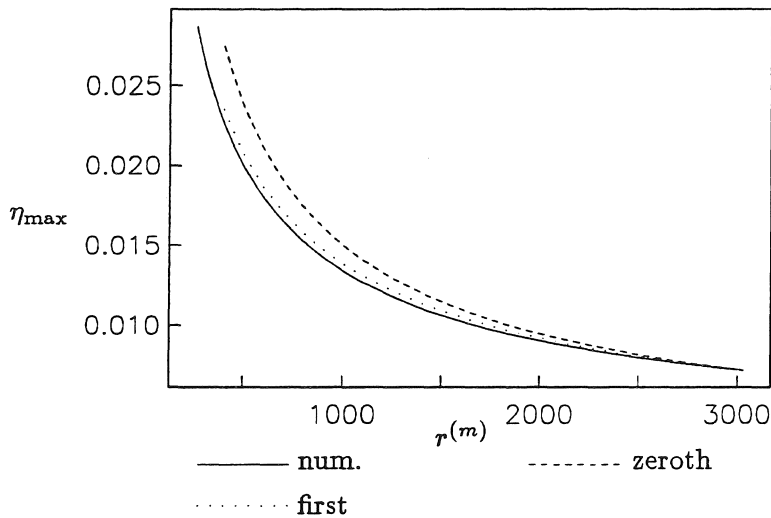


Figure 14: The total waveheight η_{\max} for a radially converging wave with initial conditions corresponding to a plane soliton solution with parameters $r_0 = 6000$, $\eta_{\max} = 0.005$. We have depicted the numerically calculated amplitude (num.), the amplitude from (91) without the leak term (zeroth) and the amplitude predicted by the complete equation (91) (first). The energy equation (91) is applied with the modified reference point $r_0 = 2999.0$, $\eta_{\max} = 0.00723$ to reduce the effect of inaccurate initial conditions.

figure 2. (see comment at the end of section 4.4) We observe that the presence of the leak term markedly improves the agreement with the numerical solution. However, it must be noted that the displayed case probably is on the limit on the validity range of the perturbation solution.

6 Concluding remarks

Numerical solutions of the Boussinesq equations confirm the existence of progressive modulations on a solitary wave like crest as predicted by standard ray theory. However, the full Boussinesq solutions inherit a pronounced damping of the modulation – a feature that cannot be reproduced by the purely hyperbolic ray equations reported previously. Corrections to the primary wave field are obtained by a two scale perturbation technique that also yields a formal derivation of the first order ray equations. In two special cases, infinitesimal modulations on a straight crest and axisymmetric focusing, we find uniform solutions of very compact form for the secondary wave field. The perturbation solution will in any case be valid for the principal crest and define boundary conditions for the diffracted wave field. However, an explicit calculation of the diffracted field is not required for the development of a corrected ray theory. Incorporating the secondary wave field in an energy balance argument for the head wave we obtain a second order transport equations that possess principally new features. One is the cross ray energy transport due to lateral velocities. Equally important are the dependence of both integrated energy density and overall wave celerity speed on the curvature of the primary crest. An energy sink, due to the diffracted waves, do also appear, but turn out to be of minor importance for the presented examples.

The new terms of the amended ray theory turn the transport equations into a mixed hyperbolic/parabolic form. Consequently the progressive modulations are damped and we observe excellent agreement with the Boussinesq equations. Also the integrated energy fluxes, cross ray velocity components and diffracted wave field approximate closely the corresponding quantities of the full solution. Very strong diffusion like damping and spreading are recognized in the numerical simulation of initially short modulations on the principal crest. Even in these cases we obtain quantitatively good results from our higher order ray theory.

The application of ray theory to fully developed wave jumps is primarily limited to weak shocks and small amplitudes. For such shocks the amended transport equations predict a finite width and, together with the detailed perturbation solution, also a diffracted wave originating from the jump zone. In the limit of weak shocks this description is found to be perfectly consistent with Miles solution for a resonant triad of solitons, with the diffracted wave as the third member. The proper reproduction of weak wave jumps is a convincing proof of the validity of the presented theory. Again we obtain quantitatively good predictions from the ray theory also for short crest transition, this time in the form a strong jump.

For axisymmetric waves our perturbation solution, although developed in a different form and organization, can be shown to be fully consistent with the results of Ko & Kuehl (1979). The new terms in the transport equations are much less important for radially converging waves. Naturally, there is no cross ray energy transport in this case. In addition, the leading contribution from the curvature dependent part of the energy density integrates to a constant in the final energy equation. However,

we obtain very good agreement with accurate numerical simulations concerning both the detailed wave profiles and the curvature dependent correction to the propagation speed, thereby establishing further confirmation of the perturbation solution.

We conclude that higher order effects in ray theory may often be important for the qualitative behavior of modulated solitary waves. A similar importance of the diffusion like effects must be expected also for other single crested “hump shaped” waves. Waves of essentially sinusoidal shape are, on the other hand, probably much less influenced since the cross ray energy transport etc. is likely to cancel over an period.

In a subsequent paper the author intend to extend the present study to involve a varying bathymetry.

Appendix:

A Numerical solution of the ray equations

Following Pedersen (1988) we use the notations δ_q and $\overline{(\)}^q$ for the divided midpoint difference and average with respect to the variable q . These operators involve two neighbouring points and give discrete approximations to the first order partial derivative and the function itself, respectively. The grid site of a quantity is denoted by subscripts for the spatial location and a single superscript for the time. When all discretization, as far as possible, is based on midpoint representations the different terms of a difference equation usually ends up with identical indices which can be said to correspond to a sort of “simulation” point for the equation. This is exploited by collecting the terms within square brackets, while leaving the indices outside.

Both the kinematic equation, (84), and the energy equation, (83), are written in a conservative form and display a mixed hyperbolic/parabolic nature. Using $e \equiv (A^{(m)})^{\frac{3}{2}}$ as a new independent variable we may write:

$$\frac{\partial e}{\partial t} = -\frac{\partial B}{\partial y} - D \quad \frac{\partial \theta}{\partial t} = -\frac{\partial G}{\partial y} \quad (102)$$

for the energy and kinematic equations respectively. The symbol D denotes the energy sink, while B and G are transport terms. Thus, apart from some of the nonlinearities and the interpretations of the unknowns, the set is of a standard type described in an almost endless array of textbooks. Consequently, there should not be need for any more than a brief documentation on the numerical method.

Contrary to the most standard textbook procedures we apply a staggered grid both in time and space and chose $e_j^{(n+\frac{1}{2})}$ and $\theta_{j+\frac{1}{2}}^{(n)}$ as unknowns. The difference equations read:

$$[\delta_t e = -\delta_y B - D]_j^{(n)} \quad (103)$$

$$[\delta_t \theta = -\delta_y G]_{j+\frac{1}{2}}^{(n+\frac{1}{2})} \quad (104)$$

where the fluxes are represented according to

$$[B = \theta \bar{e} - 3^{-\frac{3}{2}} (\bar{e}^{yt})^{-\frac{1}{3}} \delta_y \bar{e}^t]_{j+\frac{1}{2}}^{(n)} \quad (105)$$

$$G_j^{(n+\frac{1}{2})} = [\frac{1}{2} e^{\frac{2}{3}} - 3^{-\frac{1}{2}} e^{-\frac{1}{3}} \delta_y \bar{\theta}^t]_j^{(n+\frac{1}{2})} + \frac{1}{2} \bar{\theta}_j^{(n+1)} \bar{\theta}_j^{(n)} \quad (106)$$

where the meaning of the tilde depends on whether we use an up-wind scheme or not. If a symmetric scheme is used, the tilde simply denotes the midpoint average as defined in the introduction to this appendix. On the other hand, when we use the asymmetric up-wind differences in the advection terms, the tilde indicates the nearest upstream value ($\bar{e}_{j+\frac{1}{2}} = e_j$ if $\theta_{j+\frac{1}{2}} > 0$ etc.). Upstream representations have to be used whenever the last term on the right hand sides of (83) and (84) becomes very small. However, most of simulations described herein are performed with symmetric differences. The energy sink term is discretized according to:

$$[D = \frac{1}{3\sqrt{3}}(\delta_y\theta)^2 + \sqrt{3}(\delta_y(\bar{e}^{yt})^{\frac{1}{3}})^2]_{j+\frac{1}{2}}^{(n)} \quad (107)$$

At each time level the equations (103) and (104) give implicit equations for new e and θ values respectively. The former is nonlinear and is solved by an iteration technique.

References

- [1] Boussinesq, J. 1872 Théorie des ondes et des remous qui se propagent de long d'un canal rectangulaire horizontal, en commuiquant au liquide contenu dans ce canal des vitesses sensiblement pareilles de la surface au fond. *J. Math. pures appl.* (Series 2), **17**,55-108.
- [2] Cumberbach, E. Spike solution for radially symmetric solitary waves. *Phys. Fluids* **21**(3), 374-380
- [3] Friedrichs, K. O. 1948 On the derivation of the shallow water theory. Appendix to The formation of breakers and bores by J. J. Stoker. *Commun. Pure Appl. Math.* **1**, 81-85.
- [4] Funakoshi, M. 1980 Reflection of Obliquely Incident Solitary Waves. *J. Phys. Soc. Japan*, **49**(6),2371-2379.
- [5] Grimshaw, R., 1970 The solitary wave in water of variable depth. *J. Fluid. Mech.* **42**, 639-656.
- [6] Grimshaw, R. 1971 The solitary wave in water of variable depth. Part 2. *J. Fluid. Mech.* **46**, 611-622.
- [7] Knickerbocker, C. J.& Newell, A. C. 1985 Reflections from solitary waves in channels of decreasing depth. *J. Fluid Mech.* **153**, 1-16.
- [8] Ko, K. & Kuehl, H. H. 1978 Korteweg-de Vries Soliton in a Slowly Varying Medium. *Phys. Rev. Let.* **40**(4), 233-236
- [9] Ko, K. & Kuehl, H. H. 1979 Cylindrical and spherical Korteweg-deVries solitary waves. *Phys. Fluids* **22**, 1343-1348
- [10] Kulikovskii, A.G. & Reutov, V.A. 1976 Movement of solitary and periodic waves with an amplitude close to the limiting in a liquid layer of slowly varying depth. *Fluid Dyn.* **11**, 884-893.

- [11] Kulikovskii, A.G. Reutov, V.A. 1980 Propagation of nonlinear waves above semi-infinite underwater troughs and ridges. *Fluid Dyn.* **15**, 217-224.
- [12] Laitone, E. V. 1960 The second approximation to cnoidal and solitary waves. *J. Fluid Mech.* **9**, 430-444.
- [13] Liu, L.F., Yoon, S.B. 1986 Stem Waves Along a Depth Discontinuity *J. Geophys. Res.* **91** NO. C3, 3979-3982.
- [14] Longuet-Higgins, M. S. & Fenton J. D. 1974 On the mass, momentum, energy and circulation of a solitary wave II *Proc. R. Soc. Lond. A* **340**, 471-493.
- [15] Melville, W.K. 1979 On the Mach reflexion of a solitary wave. *J. Fluid Mech.* **98**, 285-297.
- [16] Miles, J.W. 1977a Obliquely interacting solitary waves. *J. Fluid Mech.* **79**, 157-169.
- [17] Miles, J.W. 1977b Resonantly interacting solitary waves. *J. Fluid Mech.* **79**, 171-179.
- [18] Miles, J.W. 1977c Diffraction of solitary waves. *Z. angew. Math. Phys.* **28**, 889-902.
- [19] Miles, J.W. 1977d An axisymmetric Boussinesq wave *J. Fluid Mech.* **84**, 181-191
- [20] Miles, J.W. 1980 Solitary waves. *Ann. Rev. Fluid Mech.* **12**, 11-43.
- [21] Pedersen G. 1988 Three-dimensional wave patterns generated by moving disturbances at transcritical speeds. *J. Fluid. Mech.* vol. **196** 39-63
- [22] Pedersen G. 1991 Finite difference representations of nonlinear waves. *Int. Journal num. meth. in fluids* **13** 671-690
- [23] Peregrine, D.H. 1983 Wave jumps and caustics in the propagation of finite-amplitude water waves. *J. Fluid Mech.* **136**, 435-452.
- [24] Peregrine, D.H. 1985 Water waves and their development in space and time. *Proc. R. Soc. Lond. A* **400**, 1-18.
- [25] Reutov, V.A. 1976 Behavior of perturbations of solitary and periodic waves on the surface of a heavy liquid. *Fluid Dyn.* **11**, 778-781.
- [26] Whitham, G.B 1974 Linear and nonlinear waves. *Pure & Applied Mathematics*
- [27] Witting, J. 1975 On the highest and other solitary waves. *SIAM J. Appl. Math.* **28**, 700-719.
- [28] Wu T.Y. 1981 Long waves in ocean and coastal waters. *Proc. ASCE, J. Eng. Mech. Div.* **107**, EM3,501-522
- [29] Yue, D.K.P. & Mei, C.C. 1980 Forward diffraction of Stokes waves by a thin wedge. *J. Fluid Mech.* **99**, 33-52.